Trap t pe an positioning ow to trap a i's pine o es using the tunne s stem

3. Phototransformation processes of emerging contaminants in surface water

Davide Vione[1] and Serge Chiron[2]

[1] *Dipartimento di Chimica Analitica, Università degli Studi di Torino, Italy*
[2] *UMR HydroSciences 5569, France*

3.1. Introduction

The transformation of dissolved organic pollutants induced by sunlight is receiving increasing attention nowadays, because these processes are expected to play a major role in natural attenuation reactions and in the formation of harmful secondary pollutants. Photochemical reactions are usually divided into direct photolysis and photosensitised transformation. In the latter case, reactive species ($^{\bullet}OH$, $^{1}O_2$, $^{3}CDOM^*$ –triplet states of Chromophoric Dissolved Organic Matter, CDOM–, $CO_3^{-\bullet}$) are produced by so-called photosensitisers (*e.g.* CDOM, nitrite and nitrate), directly or upon further reaction.[1] Direct and sensitised photolysis processes will be described in greater detail (section 2.1). Section 2.2 reports the particular case of reactions involving $^{\bullet}NO_2$. They may play a secondary role in overall pollutant degradation, but are important sources of harmful secondary pollutants (*e.g.* nitrophenols).

3.2 Direct photolysis and sensitized reactions in the transformation of emerging contaminants

3.2.1 Direct photolysis

The transformation of a compound upon direct photolysis in the environment is closely linked with its ability to absorb sunlight. Therefore, only sunlight-absorbing molecules can undergo direct photolysis in surface waters. Figure 1 below shows the processes that take place after radiation absorption.[2]

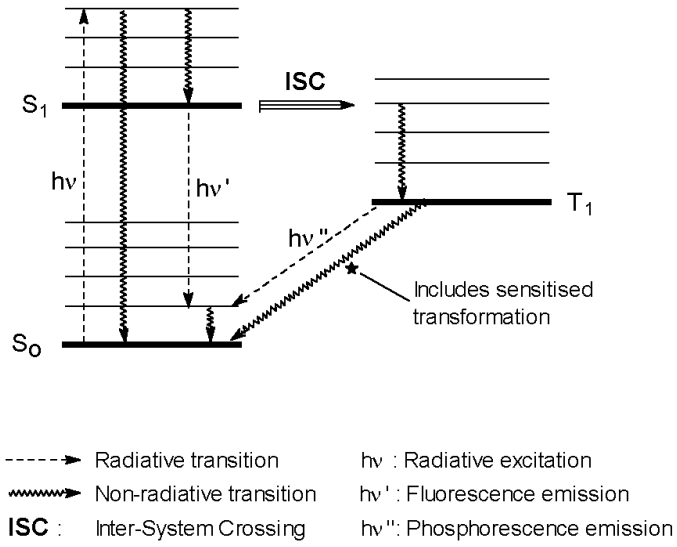

Figure 3.1. Schematic of the processes that follow the absorption of radiation by a given compound. Bold horizontal lines are electronic levels (S_o, S_1, T_1), normal-style ones represent vibrational levels for each electronic level.

Radiation absorption promotes an electron from the ground state (a singlet one for organic molecules) to an excited (singlet) state. In Figure 1, it is hypothesised that transition takes place from S_o to S_1. This may well be an oversimplification because, for instance, in the case of the UVA band of anthraquinone-2-sulphonate (absorption maximum at 333 nm) the actual transition involved is $S_o \rightarrow S_4$, while the transition probability from S_o to S_1-S_3 is extremely low.[3] Back to the case of Figure 1, the promoted electron initially reaches a vibrationally excited S_1 state, and very fast energy dissipation leads to the ground vibrational S_1 level. Several processes are possible at this stage: internal conversion to S_o, which implies loss of energy by means of *e.g.* collisions with the solvent or even chemical reactivity; emission of fluorescence radiation, which has higher wavelength (lower energy) than the excitation one (indeed, losses of vibrational energy take place throughout the process); inter-system crossing (ISC) to a triplet state (*e.g.* T_1). ISC is enabled by the fact that, although T_1 has lower energy than S_1, some vibrationally excited T_1 states can have very similar energy as ground S_1. Following ISC the electron reaches a vibrationally excited T_1 state, from which energy dissipation leads to ground T_1. In some solid systems or in deep-frozen solutions the next process could be emission of phosphorescence radiation. Under natural water conditions, collisional deactivation, energy transfer or chemical reactivity are much more likely. In the former case, energy is lost as heat. Energy transfer to other molecules could for instance induce the formation of $^1O_2$ from ground-state (triplet) O_2. A photosensitised process could follow, because $^1O_2$ is chemically reactive. As an alternative, the molecule in T_1 state could be transformed because of breaking of a chemical bond (lysis or isomerisation) or upon reaction with another molecule.

Note that T_1 is considerably longer-lived than S_1: although thermal deactivation processes may be important for the triplet state, chemical reactivity is much more likely for T_1 than for S_1.

Direct photolysis often involves some of the processes described above. However, in some cases, absorption of energetic UV radiation could lead to loss of an electron (photoionisation). The ionised molecule (usually a radical cation) is likely to react with water or some other solution components to undergo chemical transformation. In summary, direct photolysis could follow one or more of the pathways below:[4]

- **Photoionisation.** Radiation absorption causes abstraction of one electron, followed by chemical reactivity of the ionised molecule. Interestingly, photoionisation followed by reaction with H_2O can produce similar results as reaction with $^{\bullet}OH$.[5]
- **Reactions of S_1.** In some (rare) cases, the molecule in the S_1 state could undergo transformation (*e.g.* rearrangement). This can happen when S_1 is sufficiently long lived to enable chemical reactivity to occur.
- **Reactions of T_1.** Most processes of direct photolysis follow this route, which is favoured by the relatively long life of T_1.[3,4,6] The conceptually simplest ways for triplet-state reactivity would be bond-breaking, rearrangement or reaction with the solvent, but less straightforward pathways are also possible. A first possibility is energy transfer to O_2 to produce $^1O_2$, while the molecule reaches back the ground state S_o. Afterwards, $^1O_2$ could react with the molecule in the ground state (which is by far the most populated) and cause its transformation. This pathway is actually a hybrid between direct photolysis and sensitised transformation because $^1O_2$ could also react with other solution components, in which case the molecule would behave as photosensitiser. A further possibility is for T_1 to react with another solute by e^- or H-atom abstraction (T_1 states are usually oxidant). In such a case, the molecule that originally absorbed radiation (M) undergoes reduction. The compound undergoing oxidation (M') would usually undergo further transformation, but the same is not necessarily true of $M^{-\bullet}$ that could be recycled back to M by molecular oxygen:

$$M(T_1) + M'(S_o) \rightarrow M^{-\bullet} + M'^{+\bullet} \quad (1)$$

$$M'^{+\bullet} \rightarrow \text{Products} \quad (2)$$

$$M^{-\bullet} \rightarrow \text{Products} \quad (3)$$

$$M^{-\bullet} + O_2 \rightarrow M + O_2^{-\bullet} \quad (4)$$

Again at the border between direct and sensitised photolysis, this process would cause transformation of M' but not necessarily of M. Actually, such a pathway could account for the inhibition of direct photolysis carried out by non-chromophoric (*i.e.* non radiation-absorbing) Dissolved Organic Matter (DOM), which would behave as M'.[6]

A key aspect of direct photolysis is the probability for an absorbed photon to induce chemical transformation. It is called the photolysis quantum yield (Φ) and is usually measured as the ratio between the rate R of M photolysis (units of moles per litre per second, M s^{-1}) and the photon flux P_a absorbed by M (units of Einstein per litre per second, Einstein L^{-1} s^{-1}, where 1 Einstein = 1 mole

of photons). Therefore, for monochromatic radiation it is $\Phi = R\ P_a^{-1}$. For polychromatic radiation, which is the case of sunlight, the issue is a bit more complex. In the general case, the photolysis quantum yield is a function of wavelength. From the Lambert-Beer law, where A(λ) is the absorbance of the compound at the wavelength λ and $p°(\lambda)$ is the incident photon flux (sunlight), one obtains:

$$R = \int_{\lambda} \Phi(\lambda)\ p°(\lambda)[1-10^{-A(\lambda)}]\, d\lambda \qquad (5)$$

where $P_a = \int_{\lambda} p°(\lambda)[1-10^{-A(\lambda)}]\, d\lambda$. It is unfortunately not possible to derive Φ(λ) from measurements of absorbance and of reaction rates under polychromatic irradiation. Therefore, determination of Φ(λ) requires a series of irradiation experiments under monochromatic light at variable λ. The equation $\Phi = R\ P_a^{-1}$ is often applied in the case of polychromatic irradiation as well, from which one obtains the "multi-wavelength" photolysis quantum yield Φ that is a weighted average of Φ(λ) over the relevant wavelength interval.

Some examples of direct photolysis of dissolved pollutants in solution will now be reported. Direct photolysis processes have received much attention in the context of the degradation of xenobiotic compounds of high environmental concern, such as polycyclic aromatic hydrocarbons (PAHs), haloaromatics (including some pesticides and their metabolites), and more recently pharmaceuticals.[4] About PAHs, in the case of naphthalene it has been found that direct photolysis proceeds through photoionisation/deprotonation with the net loss of a H atom, followed by either oxidation to naphthoquinone, or by ring-opening with formation of monoaromatic carboxylic acids and aldehydes (Figure 2).[7]

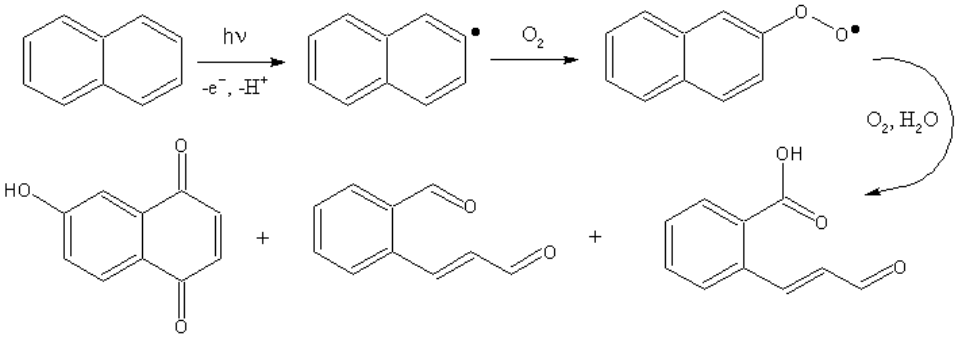

Figure 3.2. Pathways of the direct photolysis of naphthalene in aqueous solution.

Quite interestingly, quinone derivatives are more photochemically active than the parent PAHs and could undergo more extensive photoprocessing. For instance, the direct photolysis of anthracene in aerated aqueous solution yields 9,10-anthraquinone, which is able to absorb a larger fraction of sunlight compared to anthracene and undergoes photo-oxidation as a consequence (Figure 3).[8,9]

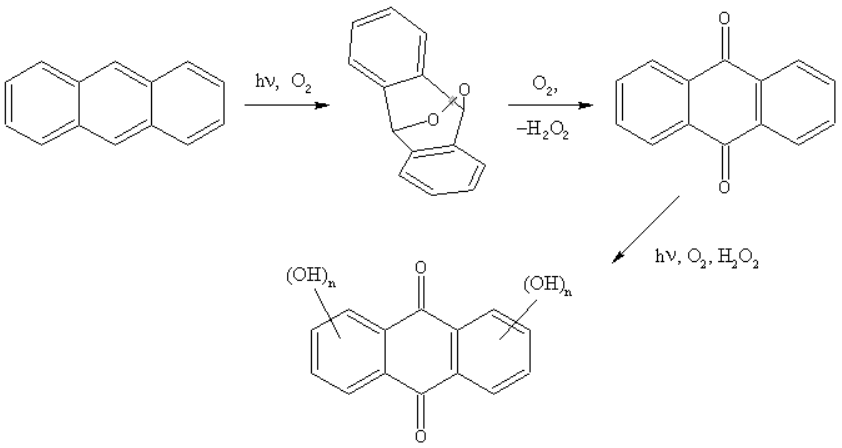

Figure 3.3. Pathways of the direct photolysis of anthracene in aqueous solution.

The photoreactivity of anthracene could be strongly substrate-dependent. Indeed, the direct photolysis of anthracene on silica proceeds via dimerisation in addition to oxidation to anthraquinone (Figure 4).[10] Furthermore, semiquinone and hydroquinone derivatives are likely to be formed upon anthraquinone reduction.[11] The surface of silica might significantly enhance photodimerisation processes compared to homogeneous aqueous solution. For instance, photodimerisation on silica (as well as photoisomerisation, photoinduced ring formation and oxidative C=C photosplitting) has been observed for *trans* 1,2-diphenylethylene (Figure 5).[12] Interestingly, SiO_2 would be a model for inorganic colloids in surface waters.[13]

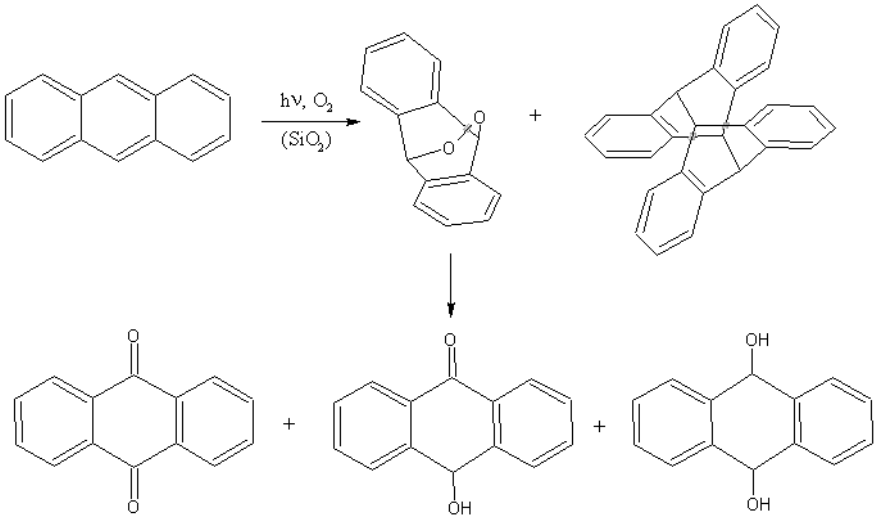

Figure 3.4. Pathways of the direct photolysis of anthracene on the surface of silica.

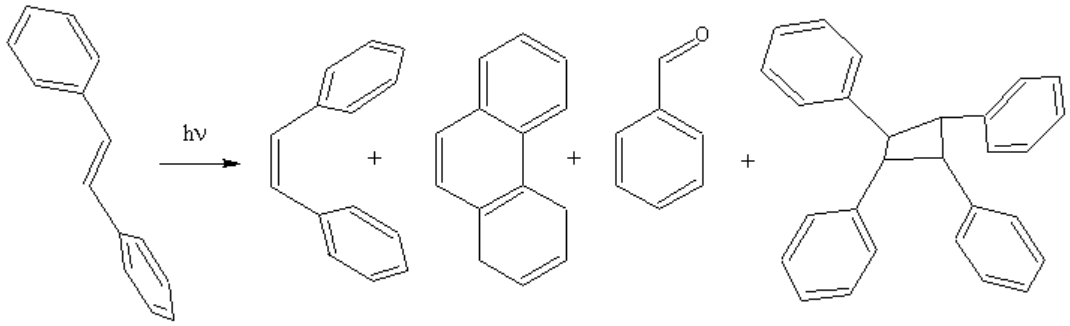

Figure 3.5. Pathways of the direct photolysis of *trans* 1,2-diphenylethylene on the surface of silica.

Chlorophenols are a class of chlorinated aromatic compounds of considerable environmental concern, because they can be released as by-products from various industrial activities.[14] Furthermore, they can be formed as secondary pollutants upon environmental transformation of various pesticides, mainly the chlorophenoxy-acetic and propionic acids [15,16] and the antimicrobial agent triclosan.[17,18] Chlorophenol direct photolysis shows an interesting difference between *ortho*- and *para*-substituted isomers. In the case of *ortho*-chlorophenols [40], the excited singlet state is sufficiently long-lived to allow chemical reactivity *via* ring contraction and loss of HCl to form a cyclopentadienyl carboxyaldehyde (Figure 6).[19] The ring-contraction process would be particularly significant for the phenolate anions.[20] In contrast, the excited triplet state would mainly react by dechlorination, either reductive (with the participation of $HO_2^{\bullet}/O_2^{-\bullet}$) to give the corresponding phenol, or involving oxygen with the final formation of dihydroxyphenols and quinones.[21] Such a process would take place with both *ortho*- and the *para*-chlorophenols (Figures 6,7).

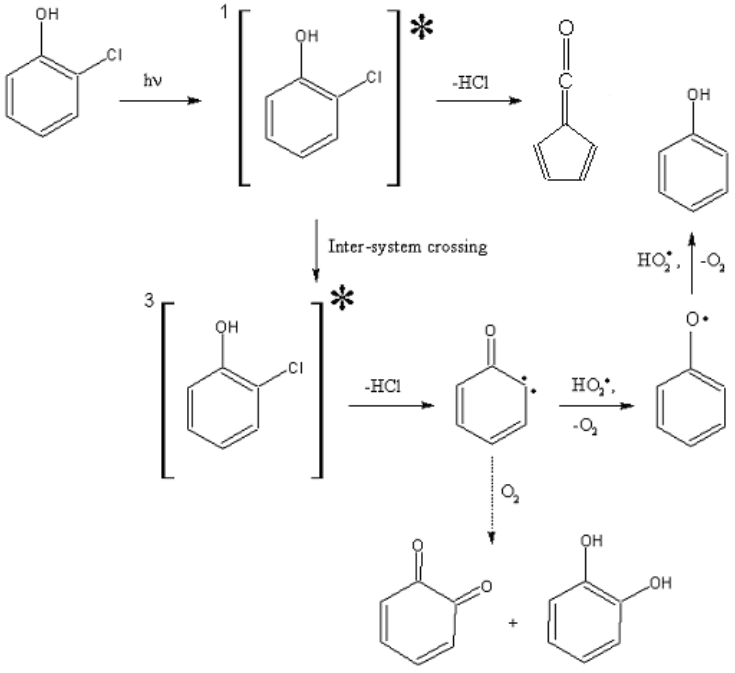

Figure 3.6. Processes involved in the direct photolysis of 2-chlorophenol in aqueous solution.

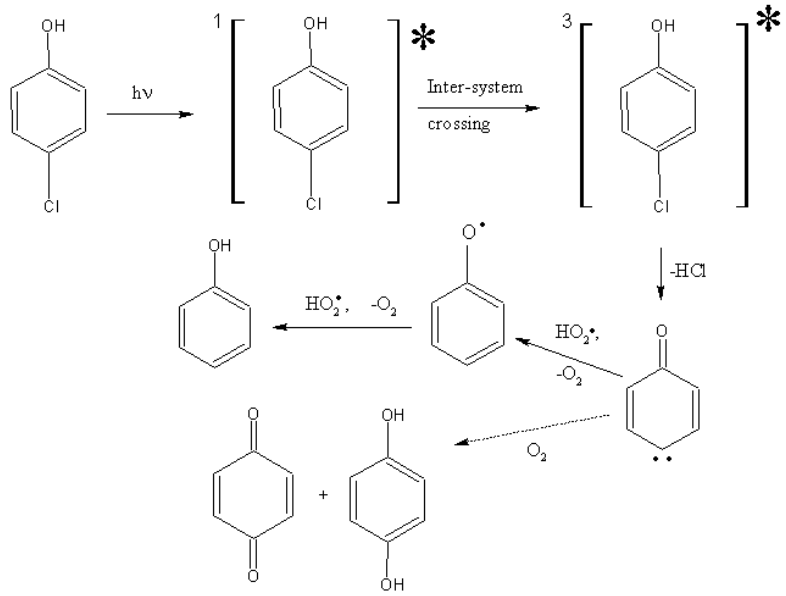

Figure 3.7. Processes involved in the direct photolysis of 4-chlorophenol in aqueous solution.

Many xenobiotic compounds of environmental concern undergo different photolysis processes in their protonated or deprotonated form, such as the herbicide 2-methyl-4-chlorophenoxyacetic acid (MCPA). The photolysis pathways are, therefore, strongly dependent on pH. In the case of MCPA the protonated form undergoes molecular rearrangement, while the anionic one follows a dechlorination-hydroxylation pathway (Figure 8).[22]

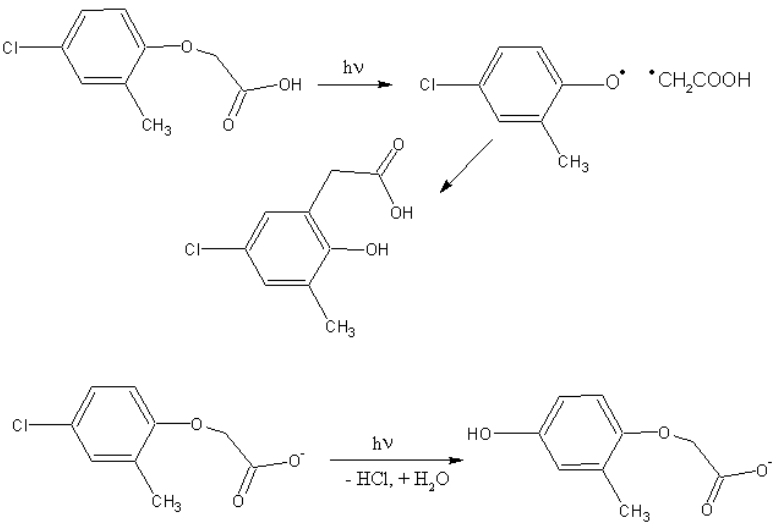

Figure 3.8. Processes involved in the direct photolysis of MCPA in aqueous solution (both neutral and anionic forms).

Dichlorprop, 2-(2,4-dichlorophenoxy)propionic acid, an herbicide extensively used in flooded rice farming, is a precursor of various chlorinated phenols in the environment, such as 4-chlorocatechol by direct photolysis (Figure 9)[23] and 2,4-dichlorophenol upon hydrolysis in aqueous solution.[24]

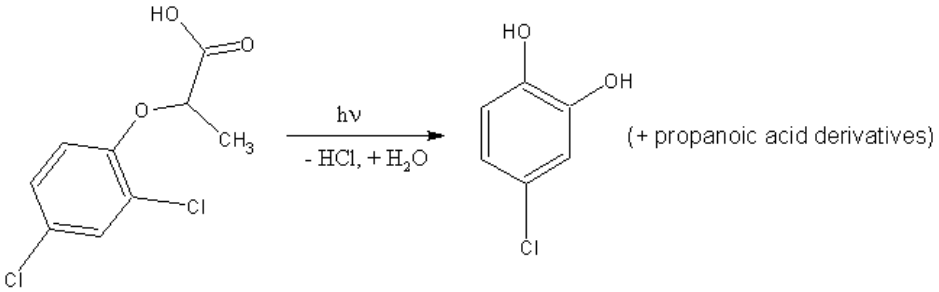

Figure 3.9. Processes involved in the direct photolysis of dichlorprop in aqueous solution.

Other xenobiotic compounds that can undergo direct photolysis in surface waters are the pesticide dicamba (Figure 10)[25] and the antimicrobial agent triclosan (Figure 11).[26] The case of triclosan is particularly interesting because its photocyclisation produces a dichlorodibenzodioxin.[27]

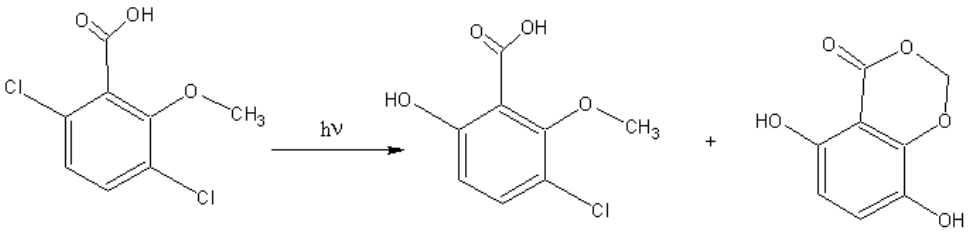

Figure 3.10. Processes involved in the direct photolysis of dicamba in aqueous solution.

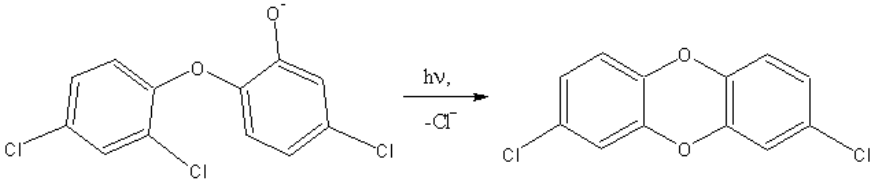

Figure 3.11. Processes involved in the direct photolysis of triclosan in aqueous solution.

The case of triclosan is a good example of a photolysis process that yields an intermediate that is more harmful than the parent compound. This finding is even more significant, because direct photolysis is the main sink of triclosan in surface waters.[26] Indeed, the photodegradation of a pollutant is not always beneficial to the environment, and the environmental and health impact of transformation intermediates is to be considered as well.[28,29] Another interesting example is the direct photolysis of the anti-epileptic drug carbamazepine that yields, among other intermediates, mutagenic acridine (Figure 12).[5,30,31]

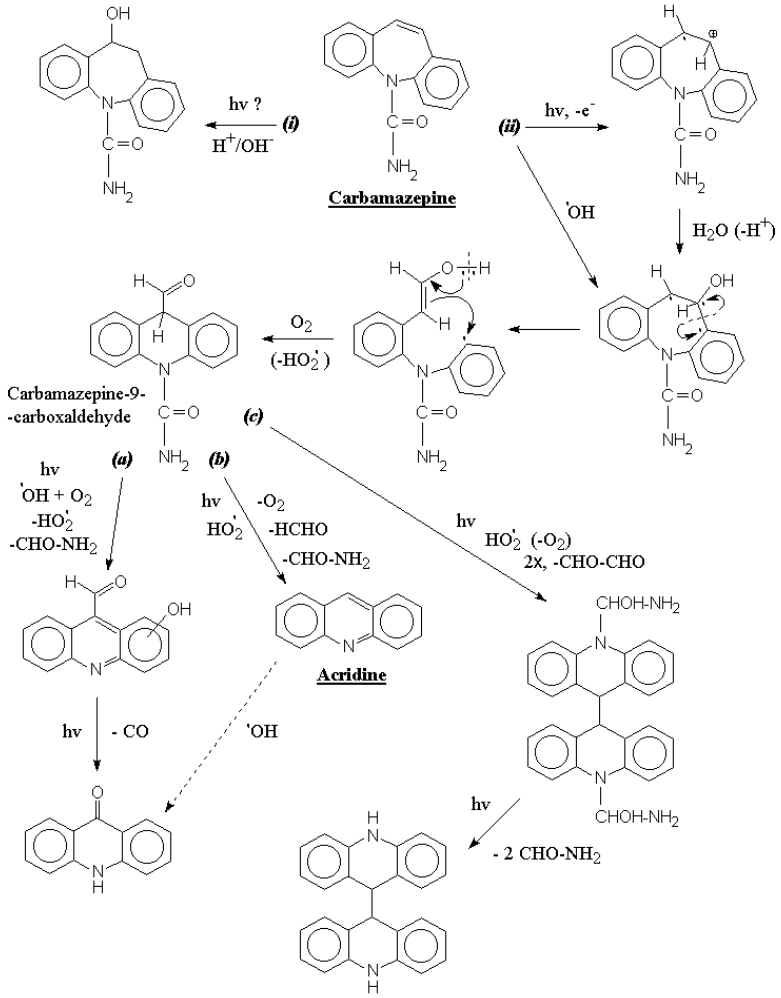

Figure 3.12. Processes involved in the direct photolysis of carbamazepine in aqueous solution.

In summary, direct photolysis can be an important process in the degradation of sunlight-absorbing compounds in surface waters, depending on the irradiation intensity (which is maximum in shallow and clear water bodies), the extent of sunlight absorption by the molecule under consideration, and the photolysis quantum yield. The disappearance of the initial molecule is not necessarily the end of the story, however, because transformation intermediates can be formed having different properties, and sometimes being more harmful than the parent compound.[32,33]

3.2.2 Reaction with •OH

Hydroxyl radicals are formed in surface waters upon irradiation of nitrate, nitrite and CDOM.[4,34] In some environments Fe(III) compounds have been shown to play a significant role as •OH sources,[35,36] but their overall significance is still unclear.[37] In particular, it is not yet clearly understood if and to what extent the complexes between Fe(III) and organic compounds are involved in the photochemical formation of •OH that is attributed to CDOM. The possible role of H_2O_2 photolysis as •OH source has been debated, but it seems established that photo-Fenton

reactions would be the main (though disputed) process by which H_2O_2 could contribute to $^{\bullet}OH$ formation in natural waters.[4,35] A recent study has shown that some ^{3}CDOM*-like triplet states would be able to oxidise water to $^{\bullet}OH$,[38] but the alternative hypothesis of $^{\bullet}OH$ formation via photo-Fenton reactions involving complexes between Fe(III) and organic compounds has to be considered.[4] It is also possible that a mixture of both pathways is operational. Therefore, while photochemical reactions of nitrate and nitrite are quite well understood,[4] several and still uncertain options are proposed as far as CDOM is concerned.

$$NO_3^- + h\nu + H^+ \rightarrow {}^{\bullet}OH + {}^{\bullet}NO_2 \quad (6)$$

$$NO_2^- + h\nu + H^+ \rightarrow {}^{\bullet}OH + {}^{\bullet}NO \quad (7)$$

$$DOM + h\nu \rightarrow {}^1DOM^* \text{ — (ISC)} \rightarrow {}^3DOM^* \quad (8)$$

$$^3DOM^* + H_2O \rightarrow [DOM+H]^{\bullet} + {}^{\bullet}OH \quad (9)$$

$$Fe^{III}\text{-}L + h\nu \rightarrow Fe^{2+} + L^{+\bullet} \quad (10)$$

$$Fe^{2+} + H_2O_2 \rightarrow Fe^{3+} + {}^{\bullet}OH + OH^- \quad (11)$$

$$FeOH^{2+} + h\nu \rightarrow Fe^{2+} + {}^{\bullet}OH \quad (12)$$

After photochemical formation, $^{\bullet}OH$ can be consumed by several water components such as DOM, carbonate, bicarbonate, bromide and nitrite. DOM is certainly the main $^{\bullet}OH$ sink in freshwater,[37] while bromide would play a major role in seawater.[4] The roles of HCO_3^-, CO_3^{2-} and NO_2^- as $^{\bullet}OH$ sinks will be discussed later, because of the potential environmental importance of consecutive reactions. The efficient $^{\bullet}OH$ scavenging by DOM in freshwater and by bromide in seawater considerably limits the ability of the $^{\bullet}OH$ radical to oxidise dissolved pollutants. This is not due to a lack in reactivity, but rather to the relatively low steady-state concentration of $^{\bullet}OH$ in surface waters that is caused by fast scavenging reactions.

The efficient scavenging of $^{\bullet}OH$ by several water components is directly linked to $^{\bullet}OH$ reactivity, because this species undergoes fast and little selective reactions with a very wide variety of organic and inorganic compounds.[39] Elevated $^{\bullet}OH$ reactivity is partially accounted for by its very high reduction potential (around 2.6 V), but thermodynamic issues only tell a limited part of the story. For instance, the sulphate radical $SO_4^{-\bullet}$ has a reduction potential that is comparable and even slightly higher than $^{\bullet}OH$,[40] but its second-order reaction rate constants with organic compounds are often lower.[39,41] Figures 13 and 14 report the second-order reaction rate constants of $^{\bullet}OH$ and $SO_4^{-\bullet}$ with two compound classes (benzoates and anisoles), where the substituent(s) in *meta* and *para* position on the aromatic ring (*ortho* substituents are excluded due to possible and confounding steric effects) are described by the corresponding Hammett σ values.[42]

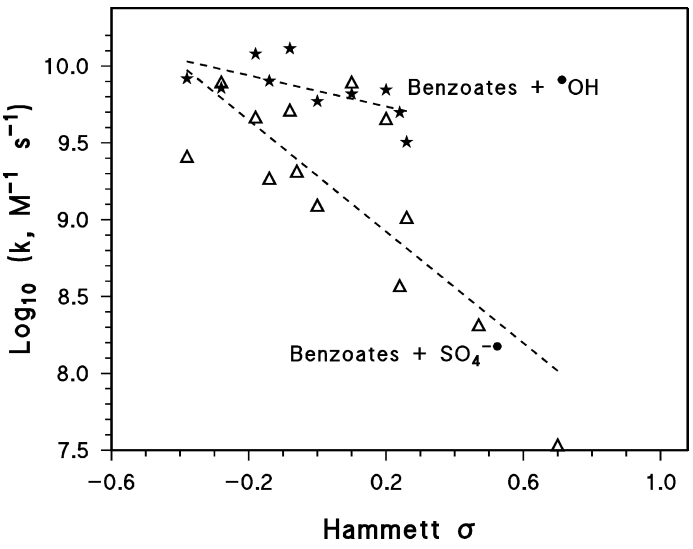

Figure 3.13. Correlation between the decimal logarithms of the second-order rate constants *k* and the Hammett σ for substituted benzoates, for reaction with the radicals $^{\bullet}OH$ and $SO_4^{-\bullet}$.

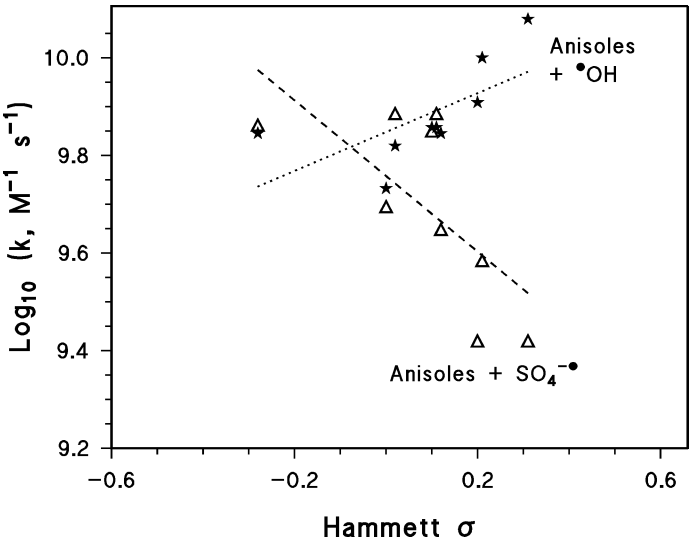

Figure 3.14. Correlation between the decimal logarithms of the second-order rate constants *k* and the Hammett σ for substituted anisoles, for reaction with the radicals $^{\bullet}OH$ and $SO_4^{-\bullet}$.

The trend of the reaction rate constants with $SO_4^{-\bullet}$ shows a statistically significant correlation of $\log_{10}(k)$ *vs.* σ in both cases, and the decrease of $\log_{10}(k)$ with increasing σ suggests that $SO_4^{-\bullet}$ reactivity is hampered by electron-withdrawing substituents. This issue is motivated by the fact that $SO_4^{-\bullet}$ only takes part in electron-abstraction processes ($SO_4^{-\bullet} + e^- \rightarrow SO_4^{2-}$) that closely follow the Hammett σ as far as reactivity is concerned. In contrast, there is no statistically significant correlation of $\log_{10}(k)$ *vs.* σ for $^{\bullet}OH$, and Figures 13,14 clearly suggest that $^{\bullet}OH$ reactions follow

poorly or not at all the Hammett σ rule. Moreover, in the case of $^{\bullet}OH$ the *k* values are all around 10^{10} M^{-1} s^{-1}, which are comparable to the $SO_4^{-\bullet}$ ones for the strongest electron-donating substituents, but that can be up to two orders of magnitude higher than for $SO_4^{-\bullet}$ in the case of electron-withdrawing ones.[42] The most likely reason for the difference between $^{\bullet}OH$ and $SO_4^{-\bullet}$ is that $^{\bullet}OH$ can follow several reaction pathways, while $SO_4^{-\bullet}$ can follow only one. Therefore, $^{\bullet}OH$ could avoid kinetic bottlenecks of e^- abstraction that may be present with some molecules, simply by reacting *via* another pathway. The main processes in which $^{\bullet}OH$ is involved are as follows:[39]

- Electron abstraction ($^{\bullet}OH + e^- \rightarrow OH^-$).
- H-atom abstraction (R-H + $^{\bullet}OH \rightarrow R^{\bullet} + H_2O$).
- Addition to double bonds (>C=C< + $^{\bullet}OH \rightarrow$ >C-C$^{\bullet}$(OH)-).
- Addition to aromatic rings.

Despite the problems connected with scavenging, reactions involving $^{\bullet}OH$ have a considerable advantage as far as formation of secondary pollutants is concerned. Indeed, photochemistry can cause effective transformation of a primary pollutant, but can sometimes form intermediates that are more toxic than the primary compound. In the case of $^{\bullet}OH$, formation of harmful pollutants is usually lower compared to other photochemical pathways (most notably direct photolysis), which accounts for the extensive exploitation of $^{\bullet}OH$ as reactive species in Advanced Oxidation Processes for water and wastewater treatment.[4]

3.2.3 Reaction with $CO_3^{-\bullet}$

The carbonate radical, $CO_3^{-\bullet}$, is produced in surface waters upon oxidation by $^{\bullet}OH$ of carbonate and bicarbonate,[39] and upon reaction between carbonate and ^{3}CDOM*.[43] Photochemical modelling suggests that reactions involving $^{\bullet}OH$ would usually prevail over ^{3}CDOM*,[43,44] thus formation of $CO_3^{-\bullet}$ in surface waters would mostly be a by-product of $^{\bullet}OH$ scavenging.

Interestingly, bicarbonate is usually more concentrated than carbonate in surface waters, but reaction between $^{\bullet}OH$ and carbonate is considerably faster. Therefore, the relative roles of carbonate and bicarbonate as $CO_3^{-\bullet}$ sources would mostly depend on solution pH. Figure 15 reports such a comparison, showing that bicarbonate oxidation would be the main $CO_3^{-\bullet}$ source below pH 8.5 (that is, in the majority of cases of environmental significance). Conversely, carbonate oxidation is more important at pH > 8.5.[37] The Figure also shows that inorganic carbon (mostly HCO_3^- + CO_3^{2-}, because H_2CO_3/CO_2 reacts quite slowly with $^{\bullet}OH$) often accounts for less than 10% of the total $^{\bullet}OH$ scavenging in freshwater, the remainder being largely accounted for by DOM.[37]

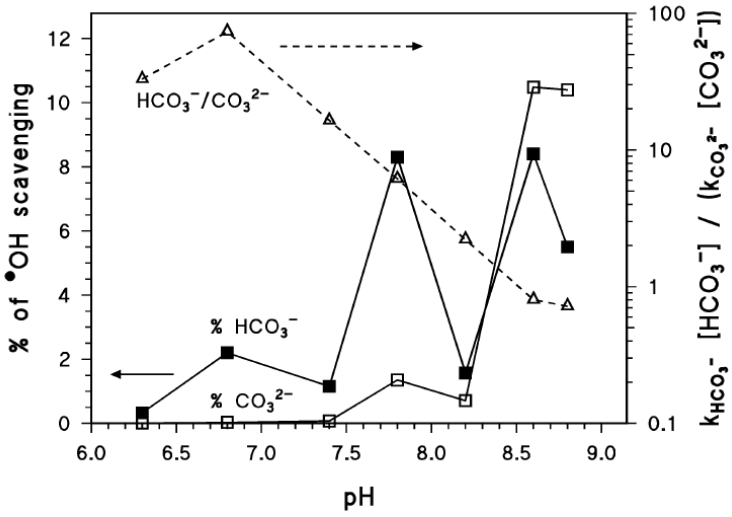

Figure 3.15. Role of carbonate and bicarbonate as $^{\bullet}OH$ scavengers. The ratio of their contributions to $^{\bullet}OH$ scavenging is also reported (note the logarithmic scale on the right Y axis).

The main $CO_3^{-\bullet}$ sink in surface freshwaters is reaction with DOM, which is considerably slower than reaction between DOM and $^{\bullet}OH$. Previous discussion of the main $CO_3^{-\bullet}$ sources suggests that the formation rate of $CO_3^{-\bullet}$ would often be an order of magnitude lower (or even less) than the $^{\bullet}OH$ formation rate (note that all transients such as $^{\bullet}OH$ are in steady-state in surface waters, thus their formation rate is equal to the rate of scavenging). However, because the average reaction rate constant between $^{\bullet}OH$ and DOM is over two orders of magnitude higher than the rate constant of $CO_3^{-\bullet}$ with DOM, the resulting $[CO_3^{-\bullet}]$ values are one-two orders of magnitude higher than the $[^{\bullet}OH]$ ones in surface waters.[44] The higher steady-state concentration of $CO_3^{-\bullet}$ compared to $^{\bullet}OH$ is largely compensated for by lower reactivity of $CO_3^{-\bullet}$. Therefore, for many xenobiotic compounds, the reaction with $CO_3^{-\bullet}$ in surface waters is negligible compared to $^{\bullet}OH$. Major exceptions are some aromatic amines (*e.g.* aniline), as well as organic sulphides and mercapto compounds.[43,45]

A suitable approach to assess the reactivity of $CO_3^{-\bullet}$ with an organic compound implies the addition of bicarbonate to nitrate under irradiation. Nitrate photolysis yields $^{\bullet}OH + ^{\bullet}NO_2$ inside a cage of water molecules, and the two photofragments can either recombine (geminate recombination) or diffuse into the solution bulk. If carbonate and bicarbonate are added at sufficiently high concentration, they react not only with bulk but also with cage $^{\bullet}OH$, thereby inhibiting geminate recombination. Indeed, compared with nitrate alone, the nitrate + bicarbonate system under irradiation yields a higher amount of a less reactive species ($CO_3^{-\bullet}$ *vs.* $^{\bullet}OH$, see scheme below). The consequences on the degradation rates of dissolved compounds closely depend on substrate reactivity toward $CO_3^{-\bullet}$ *vs.* $^{\bullet}OH$. Briefly, the degradation of compounds that would react significantly with $CO_3^{-\bullet}$ in surface waters is enhanced by addition of bicarbonate to nitrate (compared to a phosphate buffer at equal pH). Conversely, degradation of compounds that are unreactive toward $CO_3^{-\bullet}$ is inhibited by bicarbonate addition.[46]

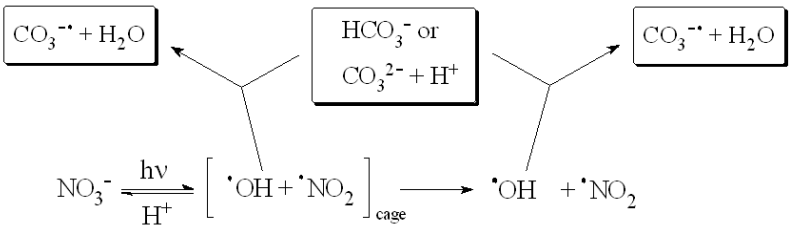

Figure 16 reports the $\log_{10}(k)$ *vs.* σ (Hammett) plot for $CO_3^{-\bullet}$ in the case of phenolates and anilines. The good linear trends suggest that reactivity with $CO_3^{-\bullet}$ is heavily influenced by the nature of substituents on the aromatic ring.

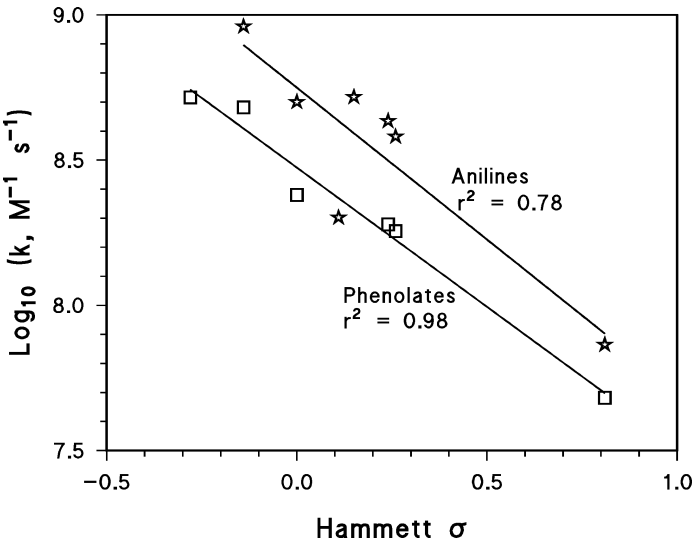

Figure 3.16. Correlation between the decimal logarithms of the second-order rate constants *k* and the Hammett σ for substituted phenolates and anilines, for reaction with the radical $CO_3^{-\bullet}$.

*3.2.4 Reaction with ^{3}CDOM**

The triplet states ^{3}CDOM* are a key player in the photochemistry of surface waters. They are a major source of $^1O_2$ (*vide infra*) and possibly of $^\bullet$OH, and they are reactive on their own. In particular, ^{3}CDOM* have a major role in the environmental degradation of phenolic compounds and of sulphonylurea herbicides.[47,48] Due to the relatively limited studies on ^{3}CDOM* reactivity that have been carried out so far compared with other transients, the list of compounds or compound classes that undergo most environmental transformation upon reaction with ^{3}CDOM* is expected to increase.

The formation of ^{3}CDOM* takes place upon radiation absorption by CDOM, followed by inter-system crossing (ISC). The main processes that could follow ^{3}CDOM* formation are thermal deactivation, reaction with O_2 to form $^1O_2$, and reaction with dissolved compounds (P).

$$CDOM + h\nu \rightarrow {}^1CDOM^* \text{—(ISC)}\rightarrow {}^3CDOM^* \qquad (13)$$

$^3CDOM^* \rightarrow CDOM$ (14)

$^3CDOM^* + O_2 \rightarrow CDOM + {}^1O_2$ (15)

$^3CDOM^* + P \rightarrow CDOM^{-\bullet} + P^{+\bullet}$ (16)

$\rightarrow (CDOM+H)^{\bullet} + (P\text{-}H)^{\bullet}$ (17)

Triplet states ^{3}CDOM* are effective oxidants and can be involved into e^- and H-atom abstraction processes. Reactions (14,15) would be the main sinks of ^{3}CDOM* in surface waters, and a pseudo-first order decay rate constant $k \sim 5 \cdot 10^5$ s^{-1} has been observed in aerated solution.[47,48]

The main issue concerning ^{3}CDOM* is that it is not a single or definite reactive species. Rather, the observed reactivity between a substrate and ^{3}CDOM* is a lumped one that results from contributions of several different reactive transients. For this reason, measurement of the second-order reaction rate constant between a xenobiotic compound and ^{3}CDOM* is very tough, and model molecules that would be representative of CDOM are often employed. The choice of CDOM proxies is mainly oriented toward compounds that are photoreactive and naturally occur in CDOM, such as aromatic carbonyls [43] and quinones (mostly anthraquinones).[3,49] Among quinones, anthraquinone-2-sulphonate has recently been used as a suitable model molecule for CDOM. Major advantages are that its triplet state (^{3}AQ2S*) does not produce $^{\bullet}$OH upon water oxidation or $^1O_2$ upon reaction with oxygen. This excludes major interfering species in the study of triplet-state reactivity.[50] The species ^{3}AQ2S* quickly reacts with H_2O to produce two transients (water adducts of AQ2S) that are considerably less reactive than ^{3}AQ2S* itself. Figure 17 reports a scheme that depicts the formation and evolution of ^{3}AQ2S* (AQ2S T_1), including the formation of the water adducts B and C (B has the water molecule attached to a carbonyl group, C has H_2O attached to a side aromatic ring). To avoid reaction between C and ground-state AQ2S, which introduces a complication in the kinetic system, the initial AQ2S concentration in irradiation experiments should not exceed 0.1 mM.[3]

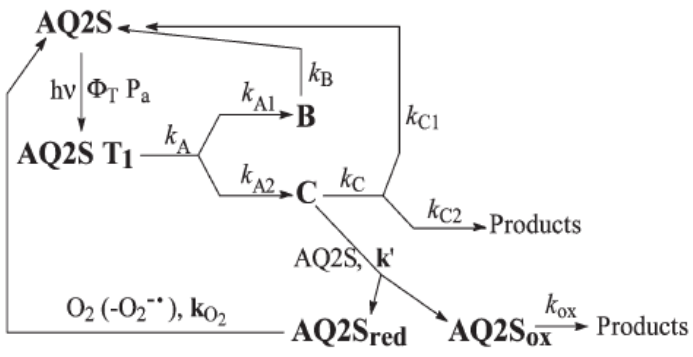

Kinetic parameter	Numerical value
Φ_T, unitless	0.18
k_A, s^{-1}	$(5.8 \pm 0.2) \times 10^6$
k_{A1}, s^{-1}	$(5.1 \pm 0.2) \times 10^6$
k_{A2}, s^{-1}	$(6.9 \pm 0.1) \times 10^5$
k_B, s^{-1}	$(2.3 \pm 0.1) \times 10^4$
k_C, s^{-1}	$(3.1 \pm 0.1) \times 10^6$
k_{C1}, s^{-1}	$(2.6 \pm 0.1) \times 10^6$
k_{C2}, s^{-1}	$(5.2 \pm 0.3) \times 10^5$
k', M^{-1} s^{-1}	$(4 \pm 1) \times 10^9$

Figure 3.17. Reaction scheme depicting the processes that follow radiation absorption by AQ2S, including formation of ^{3}AQ2S* (AQ2S T_1) and of transient water adducts (B and C). The rate constant values are reported in the table on the right.

An important issue is that phenolic antioxidants occurring in DOM can inhibit the triplet-sensitised transformation of several pollutants. The reason for this behaviour is not so much the scavenging of ^{3}CDOM* by DOM itself, but rather the re-reduction of intermediates previously oxidised by ^{3}CDOM*, back to the initial compounds (reactions 18,19; similar reaction would hold for H abstraction processes):[51,52]

$$^3\text{CDOM}^* + \text{P} \rightarrow \text{CDOM}^{-\bullet} + \text{P}^{+\bullet} \quad (18)$$

$$\text{P}^{+\bullet} + \text{DOM} \rightarrow \text{P} + \text{DOM}^{+\bullet} \quad (19)$$

3.2.5 Reaction with $^1O_2$

Singlet oxygen is formed in natural waters upon reaction between ^{3}CDOM* and O_2. Its main scavenging process is thermal deactivation upon collision with the solvent (H_2O), but competitive (although minor as far as $^1O_2$ decay is concerned) reactions with organic compounds would also occur.

$$^3\text{CDOM}^* + \text{O}_2 \rightarrow \text{CDOM} + {}^1\text{O}_2 \quad (20)$$

$$^1\text{O}_2 \rightarrow \text{O}_2 \quad (21)$$

$$^1\text{O}_2 + \text{P} \rightarrow \text{Products} \quad (22)$$

Singlet oxygen plays a very important role in the photochemical transformation of some classes of pollutants or naturally occurring molecules, such as chlorophenolates [14,53] (undissociated chlorophenols would rather react with $^{\bullet}$OH [54]) including anionic 2,4-dichloro-6-nitrophenol,[46] and aromatic amino acids such as tyrosine and histidine.[55]

An important issue concerning $^1O_2$ is the micro-heterogeneity of its distribution within CDOM: surprisingly high steady-state concentrations of $^1O_2$ have been found in hydrophobic CDOM cores compared to the solution bulk. Therefore, $^1O_2$ could play an important and still poorly recognised role in the photochemical transformation of hydrophobic pollutants, which would be preferentially located in CDOM hydrophobic cores rather than in solution.[56,57] Interestingly, no evidence has been found of a higher photochemical reactivity of CDOM particles compared to dissolved CDOM species, as far as $^1O_2$ photoproduction is concerned.[58,59] Moreover, the highest $^1O_2$ formation rates are usually found within the CDOM fractions with lower molecular weight.[60,61] A possible explanation of this apparent discrepancy is that there is little water in CDOM hydrophobic cores, which prevents reaction (21) of $^1O_2$ deactivation to take place. Therefore, $^1O_2$ in such environments could reach high steady-state concentration, despite a non-outstanding formation rate.[59]

Reactions of $^1O_2$ with organic compounds usually involve oxygenation. The following scheme reports as an instance the reaction between $^1O_2$ and furfuryl alcohol, which is a very reactive compound toward singlet oxygen and can be used as an effective $^1O_2$ probe in aqueous solution.[62]

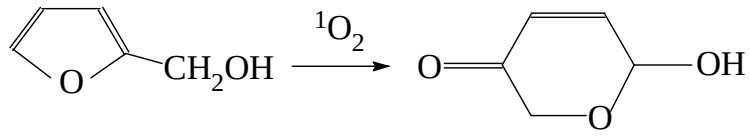

3.3 The case of photonitration

The photochemical transformation of phenolic compounds into nitrophenols in aqueous solution is a process that takes place upon reaction between the phenol and photogenerated $^{\bullet}NO_2$. The reaction is of high environmental concern because of the toxicity and potential mutagenicity of the resulting nitroderivatives.[63,64,65] The exact pathway has been under discussion for some years. It has recently been shown that the process is started by phenol oxidation by $^{\bullet}NO_2$ to produce phenoxyl radical plus HNO_2, followed by reaction between phenoxyl and another $^{\bullet}NO_2$ to yield the nitrophenol (see scheme below, where R is a generic substituent in some position of the aromatic ring).[66] Note that $^{\bullet}NO_2$ has electrophilic character, thus the nitro group will often occupy a position on the aromatic ring that is in *ortho* or *para* to the OH group (but the electron-donating or withdrawing features of the R group should also be taken into account).

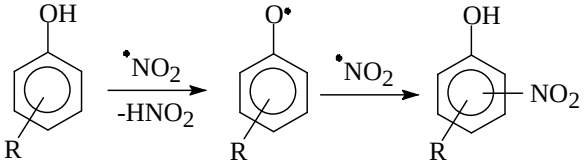

The nitration reaction of unsubstituted phenol into 2- and 4-nitrophenol has known kinetics and can be used as a probe to measure the steady-state [$^{\bullet}NO_2$] in aqueous solution. Up to now the technique has been applied to synthetic laboratory solutions, with satisfactory results.[67] The nitrating agent $^{\bullet}NO_2$ can be formed in surface waters upon photolysis of nitrate and photooxidation of nitrite.[68]

$$NO_3^- + h\nu + H^+ \rightarrow {}^{\bullet}OH + {}^{\bullet}NO_2 \qquad (23)$$

$$NO_2^- + h\nu + H^+ \rightarrow {}^{\bullet}OH + {}^{\bullet}NO \qquad (24)$$

$$NO_2^- + {}^{\bullet}OH \rightarrow {}^{\bullet}NO_2 + OH^- \qquad [k_{25} = 1\times10^{10}\ M^{-1}\ s^{-1}] \qquad (25)$$

Additional sources and sinks of $^{\bullet}NO_2$ are possible in surface waters. The oxidation of nitrite by irradiated Fe(III) (hydr)oxides is a very significant pathway leading to aromatic nitration under laboratory conditions,[69] but the assessment of its environmental importance is made problematic by the very complex speciation of Fe(III) in surface waters. An important fraction of the total Fe(III) is in fact present in the form of complexes with organic matter,[70] the (photo)reactivity of which is little known. Indeed, if the average ability of the Fe(III) species to photooxidise nitrite to $^{\bullet}NO_2$ were comparable to that of hematite, Fe(III) could be a major source of $^{\bullet}NO_2$ in surface waters containing over 1 mg Fe L^{-1}.[67] However, the extent to which hematite is representative of the photoreactivity of Fe(III) species toward nitrite is completely unknown.

It has recently been shown that a potentially important $^{\bullet}NO_2$ source in surface waters is the oxidation of nitrite by ^{3}CDOM*.[71] In particular, the reaction could be important in (C)DOM-rich waters where *e.g.* oxidation of nitrite by $^{\bullet}OH$ would be strongly inhibited by hydroxyl scavenging.

As far as the environmental importance of photonitration is concerned, the process has been shown to play an important role in the paddy fields and shallow lagoons of the Rhône river delta (S. France). In particular, nitration of 2,4-dichlorophenol (transformation intermediate arising from the herbicide dichlorprop) into 2,4-dichloro-6-nitrophenol, [67] of 4-chloro-2-methylphenol (from MCPA) into 4-chloro-2-methyl-6-nitrophenol,[72] and of 4-chlorophenol (from dichlorprop) into 4-chloro-2-nitrophenol [73] produce fairly high amounts of toxic and potentially mutagenic nitroderivatives. It has been shown that such reactions involve photogenerated $^{\bullet}NO_2$ from nitrate photolysis and nitrite oxidation.

It is possible to model the steady-state [$^{\bullet}NO_2$] in surface waters under the hypothesis that formation takes place upon nitrate photolysis and nitrite (photo)oxidation by $^{\bullet}OH$ and ^{3}CDOM*, and that hydrolysis (reactions (26,27)) is the main $^{\bullet}NO_2$ sink.[74]

$$2\ {}^{\bullet}NO_2 \rightleftarrows N_2O_4 \qquad [k_{26} = 4.5\times10^8\ M^{-1}\ s^{-1};\ k_{-26} = 6.9\times10^3\ s^{-1}] \qquad (26)$$

$$N_2O_4 + H_2O \rightarrow NO_3^- + NO_2^- + 2\ H^+ \qquad [k_{27} = 1\times10^3\ s^{-1}] \qquad (27)$$

Reaction with DOM, and in particular with its phenolic moieties, is a potential sink of nitrogen dioxide. However, at the measured levels of [$^{\bullet}NO_2$] and NPOC (Non Purgeable Organic Carbon, which is a measure of DOM) in surface waters, and given the expected rate constants for reaction between $^{\bullet}NO_2$ and phenolic compounds, DOM would be a secondary sink compared to hydrolysis. For DOM to be the main sink, it should be almost completely made up of phenolic moieties, which is very unlikely.[67,74]

From all the cited processes, it is possible to set up an approximate model for the assessment of the steady-state [$^{\bullet}NO_2$]. In the surface water layer, thereby not considering the expected decrease of [$^{\bullet}NO_2$] with depth that is caused by a decrease of sunlight irradiance, one gets equation (28):

$$[{}^{\bullet}NO_2] = \sqrt{\frac{k_{-26}+k_{27}}{2k_{26}k_{27}}\left(k_{25}[{}^{\bullet}OH][NO_2^-] + k'[{}^3CDOM^*][NO_2^-] + R_{{}^{\bullet}OH}^{NO_3^-}\right)} \qquad (28)$$

where k' = $2.3\cdot10^9$ M^{-1} s^{-1}.[71] At 22 W m^{-2} sunlight UV irradiance one gets $R_{{}^{\bullet}OH}^{NO_3^-} = 1.7\cdot10^{-7}\ [NO_3^-]$ and $[{}^{\bullet}OH] = \frac{1.7\cdot10^{-7}[NO_3^-] + 2.6\cdot10^{-5}[NO_2^-] + 5.7\cdot10^{-12}\,NPOC}{8.5\cdot10^6[HCO_3^-] + 3.9\cdot10^8[CO_3^{2-}] + 1.0\cdot10^{10}[NO_2^-] + 1.1\cdot10^{10}[Br^-] + 5.0\cdot10^4\,NPOC}$.[75] Moreover, it is $[{}^3CDOM^*] = \frac{1.3\cdot10^{-3}\,P_a^{CDOM}}{k''}$, where k'' ~ $5\cdot10^5$ s^{-1},[46] and P_a^{CDOM} = $1.9\cdot10^{-7}$ NPOC.[34] Therefore, equation (28) can be simplified as follows:

$$[{}^{\bullet}NO_2] = \sqrt{8.8\cdot10^{-9}\left(1\cdot10^{10}[{}^{\bullet}OH][NO_2^-] + 1.1\cdot10^{-6}[NO_2^-] + 1.7\cdot10^{-7}[NO_3^-]\right)} \qquad (29)$$

Under the simplified hypothesis that $[NO_3^-] \approx 200\ [NO_2^-]$, and considering the acid-base equilibrium between bicarbonate and carbonate, one also gets the following expression for [$^{\bullet}OH$], where IC = $[H_2CO_3] + [HCO_3^-] + [CO_3^{2-}]$:[75]

$$\begin{cases} [^{\bullet}OH] = \dfrac{3.1\cdot10^{-7}\cdot[NO_3^-] + 5.7\cdot10^{-12}\cdot NPOC}{\xi(IC) + 5.0\cdot10^{4}\cdot NPOC + 5.2\cdot10^{7}\cdot[NO_3^-]} \\ \xi(IC) = \dfrac{IC}{12000\cdot(10^{-10.2} + 10^{-pH})}\cdot\left(8.5\cdot10^{6}\cdot10^{-pH} + 0.025\right) \\ pH = 1.95\cdot\left(1 - 10^{-0.075\cdot IC}\right) + 6.32 \end{cases} \quad (30)$$

The cited series of approximations finally allows a manageable equation to be obtained, by which [$^{\bullet}NO_2$] can be plotted as a function of nitrite (nitrate), at the fixed ratio shown above, of NPOC and of IC. Figure 18 reports [$^{\bullet}NO_2$] *vs.* NPOC and nitrate, Figure 19 reports [$^{\bullet}NO_2$] *vs.* NPOC and IC.

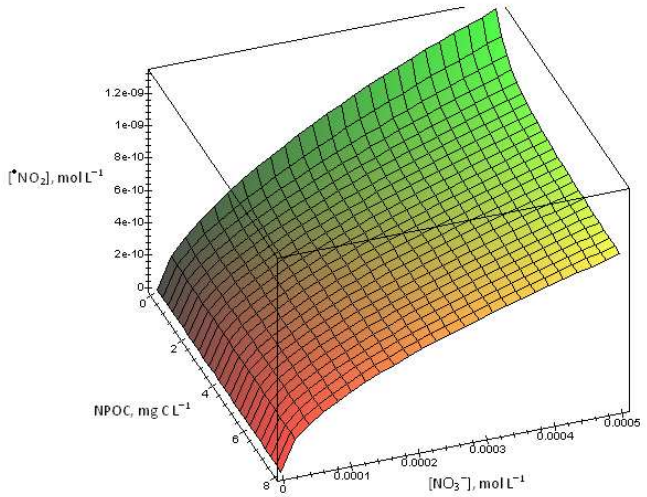

Figure 3.18. Trend of [$^{\bullet}NO_2$] as a function of nitrate and NPOC, in the presence of constant IC = 10 mg C L^{-1}. Sunlight UV irradiance: 22 W m^{-2}.

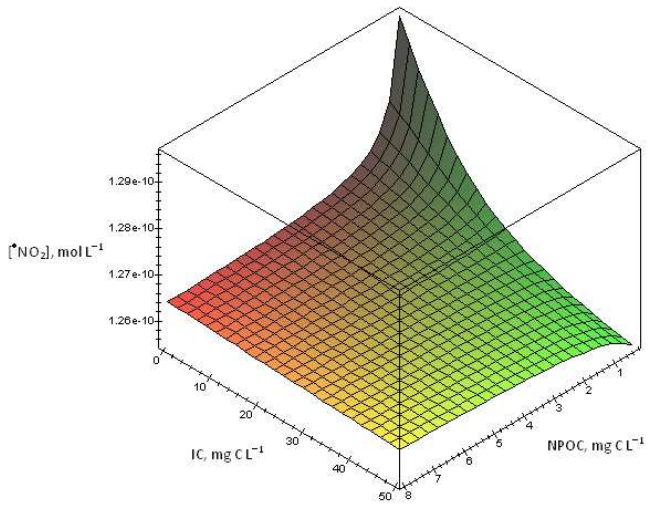

Figure 3.19. Trend of [$^{\bullet}NO_2$] as a function of IC and NPOC, in the presence of constant 10 µM nitrate. Sunlight UV irradiance: 22 W m^{-2}.

One can see that [$^{\bullet}NO_2$] obviously increases with increasing nitrate and nitrite, while it decreases with NPOC, in particular at high nitrate/nitrite. The most likely explanation is $^{\bullet}OH$ scavenging by DOM, which inhibits reaction (25). Scavenging of $^{\bullet}OH$ is also the most likely explanation of the decrease of [$^{\bullet}NO_2$] with IC. Interestingly, [$^{\bullet}NO_2$] decreases with NPOC at low IC (NPOC measures DOM that is a major $^{\bullet}OH$ scavenger), but slightly increases with NPOC at high IC. In the latter case, most $^{\bullet}OH$ is scavenged by IC and the oxidation of nitrite by ^{3}CDOM*, which would be favoured at high NPOC, could become more important as $^{\bullet}NO_2$ source.

3.4 Towards the modelling of phototransformation kinetics in surface water

It is possible to model the transformation kinetics of a substrate, a generic pollutant P, in surface water as a function of water chemistry and substrate reactivity, *via* the main photochemical reaction pathways (direct photolysis and reaction with $^{\bullet}OH$, $CO_3^{-\bullet}$, $^1O_2$ and ^{3}CDOM*). The reaction kinetics is modelled within a cylindrical volume of 1 cm^2 surface area and depth *d*. The model may use actual data of the water absorption spectrum, or it can approximate the spectrum from dissolved organic carbon (DOC) values. The model will now be described in greater detail.

3.4.1 Surface-water absorption spectrum

It is possible to find reasonable correlation between the absorption spectrum of surface waters and their content of dissolved organic matter, expressed as NPOC (Non-Purgeable Organic Carbon), which is a measure of DOM. The following equation holds for the water spectrum, referred to an optical path length of 1 cm:[34]

$$A_1(\lambda) = (0.45 \pm 0.04) \cdot NPOC \cdot e^{-(0.015 \pm 0.002)\cdot\lambda} \qquad (31)$$

As an obvious alternative, $A_1(\lambda)$ can be spectrophotometrically determined on real water samples.

3.4.2 Reaction with $^{\bullet}OH$ [34]

In natural surface waters under sunlight illumination, the main $^{\bullet}OH$ sources are (in order of average importance) Chromophoric Dissolved Organic Matter (CDOM), nitrite, and nitrate. All these species produce $^{\bullet}OH$ upon absorption of sunlight. The calculation of the photon fluxes absorbed by CDOM, nitrate and nitrite requires taking into account the mutual competition for sunlight irradiance, also considering that CDOM is the main absorber in the UV region where nitrite and nitrate absorb radiation as well. At given wavelength λ, the ratio of the photon flux densities absorbed by two different species is equal to the ratio of the respective absorbances. The same is also true of the ratio of the photon flux density absorbed by species to the total photon flux density absorbed by the solution, $p_a^{tot}(\lambda)$.[76] Accordingly, the following equations hold for the different $^{\bullet}OH$ sources (note that $A_1(\lambda)$ is the specific absorbance of the surface water layer over a 1 cm optical

path length, in units of cm^{-1}; d is the water column depth in m; $A_{tot}(\lambda)$ the total absorbance of the water column, and $p°(\lambda)$ the spectrum of sunlight):

$$A_{tot}(\lambda) = 100\, A_1(\lambda) \cdot d \quad (32)$$

$$A_{NO3-}(\lambda) = 100\, \varepsilon_{NO3-}(\lambda) \cdot d \cdot [NO_3^-] \quad (33)$$

$$A_{NO2-}(\lambda) = 100\, \varepsilon_{NO2-}(\lambda) \cdot d \cdot [NO_2^-] \quad (34)$$

$$A_{CDOM}(\lambda) = A_{tot}(\lambda) - A_{NO3-}(\lambda) - A_{NO2-}(\lambda) \approx A_{tot}(\lambda) \quad (35)$$

$$p_a^{tot}(\lambda) = p°(\lambda) \cdot (1 - 10^{-A_{tot}(\lambda)}) \quad (36)$$

$$p_a^{CDOM}(\lambda) = p_a^{tot}(\lambda) \cdot A_{CDOM}(\lambda) \cdot [A_{tot}(\lambda)]^{-1} \approx p_a^{tot}(\lambda) \quad (37)$$

$$p_a^{NO2-}(\lambda) = p_a^{tot}(\lambda) \cdot A_{NO2-}(\lambda) \cdot [A_{tot}(\lambda)]^{-1} \quad (38)$$

$$p_a^{NO3-}(\lambda) = p_a^{tot}(\lambda) \cdot A_{NO3-}(\lambda) \cdot [A_{tot}(\lambda)]^{-1} \quad (39)$$

An important issue is that $p°(\lambda)$ is usually reported in units of Einstein cm^{-2} s^{-1} nm^{-1} (see for instance Figure 20), thus the absorbed photon flux densities are expressed in the same units. To express the formation rates of $^{\bullet}OH$ in M s^{-1}, the absorbed photon fluxes P_a^i should be expressed in Einstein L^{-1} s^{-1}. Integration of $p_a^i(\lambda)$ over wavelength would give units of Einstein cm^{-2} s^{-1} that represent the moles of photons absorbed per unit surface area and unit time.

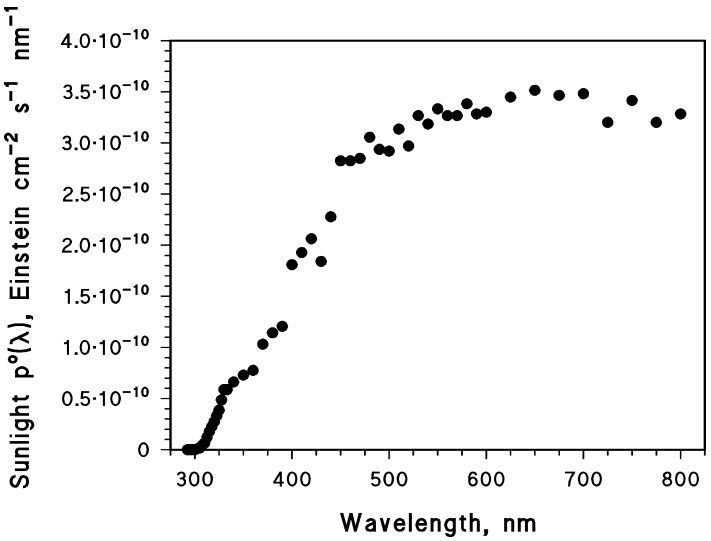

Figure 3.20. Sunlight spectral photon flux density at the water surface per unit area. The corresponding UV irradiance is 22 W m^{-2}.[77]

Therefore, assuming a cylindrical volume of unit surface area (1 cm^2) and depth d (expressed in m), the absorbed photon fluxes in Einstein L^{-1} s^{-1} units would be expressed as follows (note that 1 L = 10^3 cm^3 and 1 m = 10^2 cm):

$$P_a^{CDOM} = 10\, d^{-1} \int_{\lambda} p_a^{CDOM}(\lambda)\, d\lambda \quad (40)$$

$$P_a^{NO2-} = 10\ d^{-1} \int_{\lambda} p_a^{NO2-}(\lambda)\ d\lambda \quad (41)$$

$$P_a^{NO3-} = 10\ d^{-1} \int_{\lambda} p_a^{NO3-}(\lambda)\ d\lambda \quad (42)$$

Various studies have yielded useful correlation between the formation rate of $^{\bullet}$OH by the photoactive species and the respective absorbed photon fluxes of sunlight. In particular, it has been found that:[34,78]

$$R_{\bullet OH}^{CDOM} = (3.0 \pm 0.4) \cdot 10^{-5} \cdot P_a^{CDOM} \quad (43)$$

$$R_{\bullet OH}^{NO2-} = \int_{\lambda} \Phi_{\bullet OH}^{NO_2^-}(\lambda)\ \ p_a^{NO2-}(\lambda)\, d\lambda \quad (44)$$

$$R_{\bullet OH}^{NO3-} = (4.3 \pm 0.2) \cdot 10^{-2} \cdot \frac{[IC] + 0.0075}{2.25\,[IC] + 0.0075} \cdot P_a^{NO3-} \quad (45)$$

where [IC] = [H_2CO_3] + [HCO_3^-] + [CO_3^{2-}] is the total amount of inorganic carbon. The wavelength-dependent data of $\Phi_{\bullet OH}^{NO_2^-}(\lambda)$ are reported in Table 1.

Table 3.1. Values of the quantum yield of $^{\bullet}$OH photoproduction by nitrite, for different wavelengths of environmental significance.

λ, nm	$\Phi_{\bullet OH}^{NO_2^-}(\lambda)$	λ, nm	$\Phi_{\bullet OH}^{NO_2^-}(\lambda)$	λ, nm	$\Phi_{\bullet OH}^{NO_2^-}(\lambda)$
292.5	0.0680	315.0	0.061	350	0.025
295.0	0.0680	317.5	0.058	360	0.025
297.5	0.0680	320.0	0.054	370	0.025
300.0	0.0678	322.5	0.051	380	0.025
302.5	0.0674	325.0	0.047	390	0.025
305.0	0.0668	327.5	0.043	400	0.025
307.5	0.066	330.0	0.038	410	0.025
310.0	0.065	333.3	0.031	420	0.025
312.5	0.063	340.0	0.026	430	0.025

At the present state of knowledge it is reasonable to hypothesise that CDOM, nitrite and nitrate generate $^{\bullet}$OH independently, with no mutual interaction. Therefore, the total formation rate of $^{\bullet}$OH ($R_{\bullet OH}^{tot}$) is the sum of the contributions of the three species:

$$R_{\bullet OH}^{tot} = R_{\bullet OH}^{CDOM} + R_{\bullet OH}^{NO2-} + R_{\bullet OH}^{NO3-} \quad (46)$$

Accordingly, having as input data d, $A_1(\lambda)$, NPOC, $[NO_3^-]$, $[NO_2^-]$ and $p°(\lambda)$ (the latter referred to a 22 W m^{-2} sunlight UV irradiance, see Figure 20), it is possible to model the expected $R_{\bullet OH}^{tot}$ of the sample. The photogenerated $^\bullet$OH radicals could react either with the pollutant P or with the natural scavengers present in surface water (mainly organic matter, bicarbonate, carbonate and nitrite). The natural scavengers have an $^\bullet$OH scavenging rate constant:

$$\Sigma_i k_{Si} [S_i] = 5\times10^4 \, NPOC + 8.5\times10^6 \, [HCO_3^-] + 3.9\times10^8 \, [CO_3^{2-}] + 1.0\times10^{10} \, [NO_2^-] \quad (47)$$

($\Sigma_i k_{Si} [S_i]$ has units of s^{-1}; NPOC = non-purgeable organic carbon is a measure of DOC, expressed in mg C L^{-1}, and the other concentration values are in molarity). Accordingly, the reaction rate between the pollutant P and $^\bullet$OH can be expressed as follows:

$$R_P^{\bullet OH} = R_{\bullet OH}^{tot} \frac{k_{P,\bullet OH} [P]}{k_{P,\bullet OH} [P] + \sum_i k_{Si} [S_i]} \quad (48)$$

where $k_{P,\bullet OH}$ is the second-order reaction rate constant between P and $^\bullet$OH, and [P] is a molar concentration. Note that, in the vast majority of environmental cases it would be $k_{P,\bullet OH} [P] \ll \Sigma_i k_{Si} [S_i]$, thus the $k_{P,\bullet OH} [P]$ term can be neglected at the denominator of equation (48). The pseudo-first order degradation rate constant of P is $k_P = R_{\bullet OH}^P [P]^{-1}$, and the half-life time is $t_P = \ln 2 \, k_P^{-1}$. The time t_P is expressed in seconds of continuous irradiation under sunlight, at constant 22 W m^{-2} UV irradiance. It has been shown that the sunlight energy reaching the ground in a summer sunny day (SSD) such as 15 July at 45°N latitude corresponds to 10 h = 3.6·10^4 s of continuous irradiation at 22 W m^{-2} UV irradiance.[74] Accordingly the half-life time of P, because of reaction with $^\bullet$OH, would be expressed as follows in SSD units:

$$\tau_{P,\bullet OH}^{SSD} = \frac{\ln 2 \sum_i k_{Si} [S_i]}{3.6\cdot10^4 \, R_{\bullet OH}^{tot} \, k_{P,\bullet OH}} = 1.9\cdot10^{-5} \frac{\sum_i k_{Si} [S_i]}{R_{\bullet OH}^{tot} \, k_{P,\bullet OH}} \quad (49)$$

It is 1.9·10^{-5} = ln 2 (3.6·10^4)$^{-1}$. The steady-state [$^\bullet$OH] under 22 W m^{-2} UV irradiance would be:

$$[^\bullet OH] = \frac{R_{\bullet OH}^{tot}}{\sum_i k_{Si} [S_i]} \quad (50)$$

3.4.3 Direct photolysis [79,80]

The calculation of the photon flux absorbed by P requires taking into account the mutual competition for sunlight irradiance between P and the other surface water components (mostly CDOM, which is the main sunlight absorber in the spectral region of interest, around 300-500 nm).

Under the Lambert-Beer approximation, at a given wavelength λ, the ratio of the photon flux densities absorbed by two different species is equal to the ratio of the respective absorbances.[76] Accordingly, the photon flux absorbed by P in a water column of depth d (expressed in m) can be

obtained by the following equations (note that $A_1(\lambda)$ is the specific absorbance of the surface water sample over a 1 cm optical path length, $A_{tot}(\lambda)$ the total absorbance of the water column, $p°(\lambda)$ the spectrum of sunlight, referred to a UV irradiance of 22 W m^{-2} as per Figure 20, $\varepsilon_P(\lambda)$ the molar absorption coefficient of P, in units of M^{-1} cm^{-1}, and $p_a^P(\lambda)$ its absorbed spectral photon flux density; it is also $p_a^P(\lambda) \ll p_a^{tot}(\lambda)$ and $A_P(\lambda) \ll A_{tot}(\lambda)$ in the very vast majority of environmental cases):

$$A_{tot}(\lambda) = 100\ A_1(\lambda) \cdot d \tag{51}$$

$$A_P(\lambda) = 100\ \varepsilon_P(\lambda) \cdot d \cdot [P] \tag{52}$$

$$p_a^{tot}(\lambda) = p°(\lambda) \cdot (1 - 10^{-A_{tot}(\lambda)}) \tag{53}$$

$$p_a^P(\lambda) = p_a^{tot}(\lambda) \cdot A_P(\lambda) \cdot [A_{tot}(\lambda)]^{-1} \tag{54}$$

The absorbed photon flux P_a^P is the integral over wavelength of the absorbed photon flux density:

$$P_a^P = \int_\lambda p_a^P(\lambda)\, d\lambda \tag{55}$$

The sunlight spectrum $p°(\lambda)$ is referred to a unit surface area (units of Einstein s^{-1} nm^{-1} cm^{-2}, Figure 20), thus P_a^P (units of Einstein s^{-1} cm^{-2}) represents the photon flux absorbed by P inside a cylinder of unit area (1 cm^2) and depth $100 \cdot d$ (d is expressed in metres, thus 100 d is in cm). The rate of photolysis of P, expressed in M s^{-1}, can be expressed as follows (note that 1 L = 10^3 cm^3 and 1 m = 10^2 cm):

$$Rate_P = 10\ d^{-1} \int_\lambda \Phi_P(\lambda)\ p_a^P(\lambda)\, d\lambda \tag{56}$$

where $\Phi_P(\lambda)$ is the photolysis quantum yield of P in the relevant wavelength interval (also note that 1 L = 10^3 cm^3). The pseudo-first order degradation rate constant of P is $k_P = Rate_P\ [P]^{-1}$, which corresponds to a half-life time $t_P = ln\ 2\ (k_P)^{-1}$. The time t_P is expressed in seconds of continuous irradiation under sunlight, at 22 W m^{-2} UV irradiance. The sunlight energy reaching the ground in a summer sunny day (SSD) such as 15 July at 45°N latitude corresponds to 10 h = 3.6×10^4 s continuous irradiation at 22 W m^{-2} UV irradiance.[74] Errore. Il segnalibro non è definito. Accordingly, the half-life time expressed in SSD units would be given by:

$$\tau^{SSD}_P = (3.6 \times 10^4)^{-1}\ ln\ 2\ (k_P)^{-1} = 1.9 \times 10^{-5}\ [P]\ d\ 10^{-3}\ (\Phi_P\ P_a^{NCP})^{-1} = 1.9 \times 10^{-5}\ [NCP]\ d\ 10^{-3}\ (\Phi_{NCP} \int_\lambda p_a^{NCP}(\lambda)\, d\lambda)^{-1} = 1.9 \times 10^{-5}\ [NCP]\ d\ 10^{-3}\ (\Phi_{NCP} \int_\lambda p_a^{tot}(\lambda) \cdot A_{NCP}(\lambda) \cdot [A_{tot}(\lambda)]^{-1}\, d\lambda)^{-1} = \frac{1.9 \times 10^{-8}\ d}{\Phi_{NCP} \int_\lambda p°(\lambda)\, (1 - 10^{-A_1(\lambda)\, d})\, \frac{\varepsilon_{NCP}(\lambda)}{A_1(\lambda)}\, d\lambda} \tag{57}$$

Note that $1.9 \cdot 10^{-8} = 10^{-3}\ (\ln 2)\ (3.6 \cdot 10^4)^{-1}$.

3.4.4 Reaction with $CO_3^{-\bullet}$ [81]

The radical $CO_3^{-\bullet}$ can be produced upon oxidation of carbonate and bicarbonate by $^{\bullet}OH$, upon carbonate oxidation by $^3CDOM^*$, and possibly also from irradiated Fe(III) oxide colloids and carbonate.[82] However, as far as the latter process is concerned, there is still insufficient knowledge about the Fe speciation in surface waters to enable a proper modelling. The main sink of the carbonate radical in surface waters is the reaction with DOM.

$$^{\bullet}OH + CO_3^{2-} \rightarrow OH^- + CO_3^{-\bullet} \qquad [k_{58} = 3.9\times10^8\ M^{-1}\ s^{-1}] \qquad (58)$$

$$^{\bullet}OH + HCO_3^- \rightarrow H_2O + CO_3^{-\bullet} \qquad [k_{59} = 8.5\times10^6\ M^{-1}\ s^{-1}] \qquad (59)$$

$$^3CDOM^* + CO_3^{2-} \rightarrow CDOM^{-\bullet} + CO_3^{-\bullet} \qquad [k_{60} \approx 1\times10^5\ M^{-1}\ s^{-1}] \qquad (60)$$

$$DOM + CO_3^{-\bullet} \rightarrow DOM^{+\bullet} + CO_3^{2-} \qquad [k_{61} \approx 10^2\ (mg\ C)^{-1}\ s^{-1}] \qquad (61)$$

The formation rate of $CO_3^{-\bullet}$ in reactions (58, 59) is given by the formation rate of $^{\bullet}OH$ times the fraction of $^{\bullet}OH$ that reacts with carbonate and bicarbonate, as follows:

$$R_{CO_3^{-\bullet}}^{^{\bullet}OH} = R_{^{\bullet}OH}^{tot} \cdot \frac{8.5\cdot10^6\cdot[HCO_3^-] + 3.9\cdot10^8\cdot[CO_3^{2-}]}{5\cdot10^4\cdot NPOC + 1.0\cdot10^{10}\cdot[NO_2^-] + 8.5\cdot10^6\cdot[HCO_3^-] + 3.9\cdot10^8\cdot[CO_3^{2-}]} \qquad (62)$$

The formation of $CO_3^{-\bullet}$ in reaction (60) is given by:

$$R_{CO_3^{-\bullet}}^{CDOM} = 6.5\cdot10^{-3}\cdot[CO_3^{2-}]\cdot P_a^{CDOM} \qquad (63)$$

The total formation rate of $CO_3^{-\bullet}$ is $R_{CO_3^{-\bullet}}^{tot} = R_{CO_3^{-\bullet}}^{^{\bullet}OH} + R_{CO_3^{-\bullet}}^{CDOM}$. The transformation rate of P by $CO_3^{-\bullet}$ is given by the fraction of $CO_3^{-\bullet}$ that reacts with P, in competition with reaction (61) between $CO_3^{-\bullet}$ and DOM:

$$R_{P,CO_3^{-\bullet}} = \frac{R_{CO_3^{-\bullet}}^{tot}\cdot k_{P,CO_3^{-\bullet}}\cdot[P]}{k_{61}\cdot NPOC + k_{P,CO_3^{-\bullet}}\cdot[P]} \qquad (64)$$

where $k_{P,CO_3^{-\bullet}}$ is the second-order reaction rate constant between P and $CO_3^{-\bullet}$. In the very vast majority of environmental cases, it is $k_{P,CO_3^{-\bullet}}\ [P] \ll k_{61}\ NPOC$.

In a pseudo-first order approximation, the rate constant of P transformation is $k_P = R_{P,CO_3^{-\bullet}}\ [P]^{-1}$ and the half-life time is $t_P = ln\ 2\ k_P^{-1}$. Considering the usual conversion (≈ 10 h) between a constant 22 W m^{-2} sunlight UV irradiance and a SSD unit, the following expression for $\tau_{NCP,CO3-\bullet}^{SSD}$ is obtained:

$$\tau_{P,CO_3^{-\bullet}}^{SSD} = 1.9\cdot10^{-5}\cdot\left(\frac{k_{61}\cdot NPOC}{R_{CO_3^{-\bullet}}^{tot}\cdot k_{P,CO_3^{-\bullet}}}\right) \qquad (65)$$

Note that $1.9 \cdot 10^{-5} = \ln 2 \, (3.6 \cdot 10^4)^{-1}$.

3.4.5 Reaction with $^1O_2$ [83]

The formation of singlet oxygen in surface waters takes place upon energy transfer between ground-state molecular oxygen and the excited triplet states of CDOM (^{3}CDOM*). Accordingly, irradiated CDOM is practically the only source of $^1O_2$ in aquatic systems. In contrast, the main $^1O_2$ sink is the energy loss to ground-state O_2 by collision with water molecules, with a pseudo-first order rate constant $k_{^1O_2} = 2.5 \times 10^5$ s^{-1}. Dissolved species, including dissolved organic matter that is certainly able to react with $^1O_2$, would play a minor role as sinks of $^1O_2$ in aquatic systems. The main processes involving $^1O_2$ and P in surface waters would be the following:

$^3\text{CDOM}^* + O_2 \rightarrow \text{CDOM} + {}^1O_2$ (66)

$^1O_2 + H_2O \rightarrow O_2 + H_2O + \text{heat}$ (67)

$^1O_2 + P \rightarrow \text{Products}$ (68)

In the Rhône delta waters it has been found that the formation rate of $^1O_2$ by CDOM is $R_{^1O_2}^{CDOM} = 1.25 \cdot 10^{-3} \, P_a^{CDOM}$.[84] Considering the competition between the deactivation of $^1O_2$ by collision with the solvent (reaction 67) and reaction (68) with P, one gets the following expression for the degradation rate of P by $^1O_2$ (note that $k_{P,^1O_2} \cdot [P] \ll k_{^1O_2}$):

$$R_P^{^1O_2} = R_{^1O_2}^{CDOM} \cdot \frac{k_{P,^1O_2} \cdot [P]}{k_{^1O_2}} \quad (69)$$

In a pseudo-first order approximation, the rate constant of P transformation is $k_P = R_P^{^1O_2} \, [P]^{-1}$ and the half-life time is $t_P = \ln 2 \, k_P^{-1}$. Considering the usual conversion (≈ 10 h) between a constant 22 W m^{-2} sunlight UV irradiance and a SSD unit, the following expression for $\tau_{P,^1O_2}^{SSD}$ is obtained (remembering that $R_{^1O_2}^{CDOM} = 1.25 \cdot 10^{-3} \, P_a^{CDOM}$ and that $P_a^{CDOM} = 10^3 \, d^{-1} \int_\lambda p_a^{CDOM}(\lambda) \, d\lambda$):

$$\tau_{P,^1O_2}^{SSD} = \frac{4.81}{R_{^1O_2}^{CDOM} \, k_{P,^1O_2}} = \frac{3.85 \cdot d}{k_{P,^1O_2} \cdot \int_\lambda p_a^{CDOM}(\lambda) \, d\lambda} \quad (70)$$

Note that $3.85 = (\ln 2) \, k_{1O2} \, (1.25 \cdot 10^{-3} \cdot 3.60 \cdot 10^4 \cdot 10^3)^{-1}$.

*3.4.6 Reaction with ^{3}CDOM** [83]

The formation of CDOM excited triplet states (^{3}CDOM*) in surface waters is a direct consequence of radiation absorption by CDOM itself. In aerated solution, ^{3}CDOM* could undergo thermal deactivation or reaction with O_2, and a pseudo-first order quenching rate constant $k_{^3CDOM^*} \sim 5 \cdot 10^5$ s^{-1} has been observed. The quenching of ^{3}CDOM* would be in competition with reaction between ^{3}CDOM* and P:

$$CDOM + h\nu \rightarrow {}^3CDOM^* \quad (71)$$

$${}^3CDOM^* \text{—}(O_2)\rightarrow \text{Deactivation and } {}^1O_2 \text{ production} \quad (72)$$

$${}^3CDOM^* + P \rightarrow \text{Products} \quad (73)$$

In the Rhône delta waters it has been found that the formation rate of ^{3}CDOM* is $R_{^3CDOM^*} = 1.28 \cdot 10^{-3}\ P_a^{CDOM}$.[84] Considering the competition between reaction (73) with P and other processes (reaction 72), the following expression for the degradation rate of P by ^{3}CDOM* is obtained (note that $k_{P,^3CDOM^*} \cdot [P] \ll k_{^3CDOM^*}$, where $k_{P,^3CDOM^*}$ is the second-order reaction rate constant between P and ^{3}CDOM*):

$$R_P^{^3CDOM^*} = R_{^3CDOM^*} \cdot \frac{k_{P,^3CDOM^*} \cdot [P]}{k_{^3CDOM^*}} \quad (74)$$

In a pseudo-first order approximation, the rate constant of P transformation is $k_P = R_P^{^3CDOM^*}\ [P]^{-1}$ and the half-life time is $t_P = ln\ 2\ k_P^{-1}$. Considering the usual conversion (≈ 10 h) between a constant 22 W m^{-2} sunlight UV irradiance and a SSD unit, one gets the following expression for $\tau_{P,^3CDOM^*}^{SSD}$ (remembering that $P_a^{CDOM} = 10^3\ d^{-1} \int_\lambda p_a^{CDOM}(\lambda)\, d\lambda$):

$$\tau_{P,^3CDOM^*}^{SSD} = \frac{7.52 \cdot d}{k_{P,^3CDOM^*} \cdot \int_\lambda p_a^{CDOM}(\lambda)\, d\lambda} \quad (75)$$

Note that $7.52 = (\ln 2)\ k_{^3CDOM^*}\ (1.28 \cdot 10^{-3} \cdot 3.60 \cdot 10^4 \cdot 10^3)^{-1}$.

3.4.7 Photochemical transformation of organic pollutants

The model described so far can be used to predict the environmental persistence of dissolved molecules. In recent years, surface-water pollution by pharmaceuticals has become a considerable environmental problem, which accounts for the importance of predicting the persistence and fate of these compounds. Table 2 reports the quantum yields and rate constant values that have been determined for carbamazepine (CBZ, antiepileptic drug) and ibuprofen (IBP, analgesic) toward the main photochemical processes that are active in surface waters. Note that carbamazepine would mainly be degraded upon direct photolysis and reaction with $^\bullet$OH, while ibuprofen would react upon direct photolysis as well as with $^\bullet$OH and ^{3}CDOM*. Reactions with $^1O_2$ and $CO_3^{-\bullet}$ would be insignificant for both compounds.[85,86]

Table 3.2. Parameters describing the photochemical reactivity of CBZ and IBP, toward processes that are relevant to surface waters.

	Carbamazepine	**Ibuprofen**
Φ_P (polychromatic, UVB)	$(7.8\pm1.8)\cdot10^{-4}$	0.33±0.05
$k_{P,^{\bullet}OH}$, $M^{-1}s^{-1}$	$(1.8\pm0.2)\cdot10^{10}$	$(1.0\pm0.3)\cdot10^{10}$
$k_{P,^3CDOM*}$, $M^{-1}s^{-1}$	$(7.0\pm0.2)\cdot10^{8}$	$(9.7\pm0.2)\cdot10^{9}$
$k_{P,^1O_2}$, $M^{-1}s^{-1}$	$(1.9\pm0.1)\cdot10^{5}$	$(6.0\pm0.6)\cdot10^{4}$

The following plots report the modelled half-life times of CBZ and IBP as a function of water depth and chemical composition (NPOC, nitrite and carbonate).

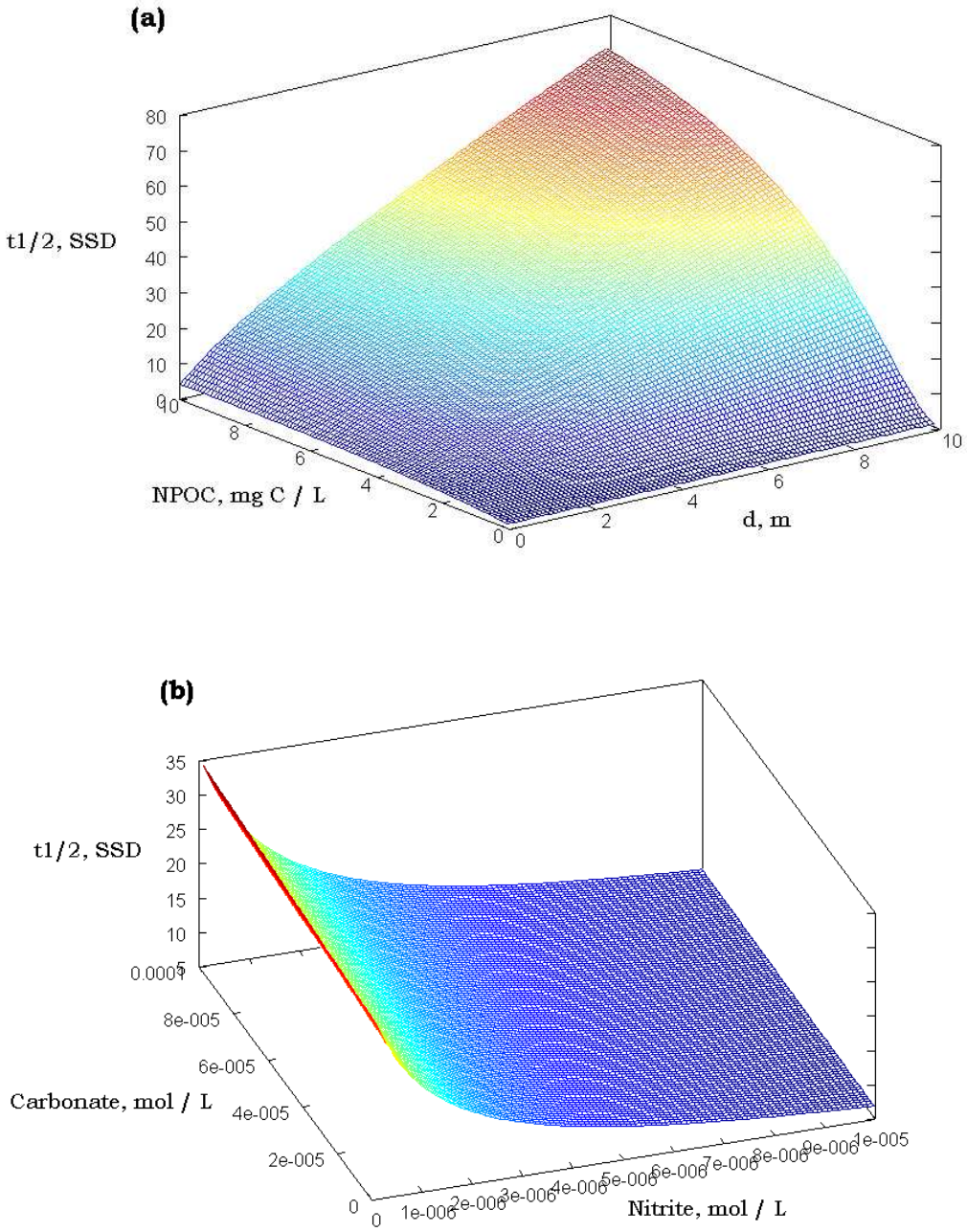

Figure 3.21. Half-life time of CBZ as a function of: **(a)** NPOC and depth, with constant 50 µM nitrate, 1 µM nitrite, 2 mM bicarbonate and 10 µM carbonate. **(b)** Carbonate and nitrite, with constant 5 m depth, 3 mg C / L NPOC, 50 µM nitrate and 2 mM bicarbonate.

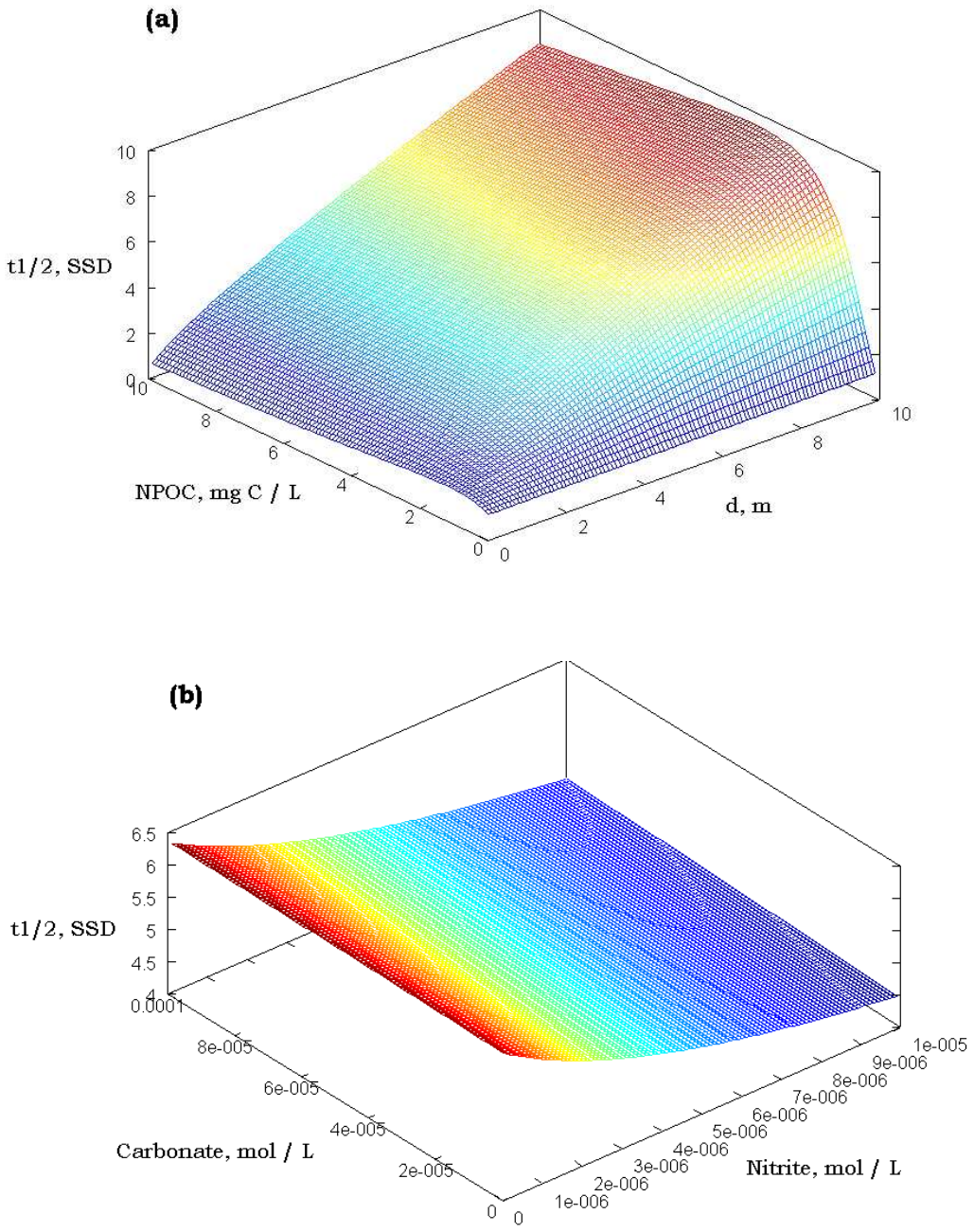

Figure 3.22. Half-life time of IBP as a function of: **(a)** NPOC and depth, with constant 50 µM nitrate, 1 µM nitrite, 2 mM bicarbonate and 10 µM carbonate. **(b)** Carbonate and nitrite, with constant 5 m depth, 3 mg C / L NPOC, 50 µM nitrate and 2 mM bicarbonate.

First of all, CBZ would be more persistent than IBP in surface waters. The half-life time of CBZ increases with increasing depth, NPOC and carbonate, and decreases with increasing nitrite. The depth effect is caused by sunlight irradiance that decreases with depth. Moreover, NPOC scavenges

$^{\bullet}$OH and competes with CBZ for irradiance, thereby inhibiting both $^{\bullet}$OH reaction and direct photolysis. Finally, carbonate scavenges $^{\bullet}$OH, and nitrite produces it.

As far as IBP is concerned, its half-life time has a maximum as a function of NPOC, because reaction with $^{\bullet}$OH prevails at low NPOC and reaction with ^{3}CDOM* at high NPOC. The increase of the half-life time with increasing depth is due to the fact that the deeper layers of a water body are poorly illuminated and, therefore, do not constitute a good environment for photochemical reactions to take place. The increase of the half-life time with increasing carbonate and the decrease with nitrite is accounted for by the fact that CO_3^{2-} is an $^{\bullet}$OH scavenger that inhibits the hydroxyl-related pathway of IBP transformation, with nitrite is an $^{\bullet}$OH source that causes the opposite effect.

The model approach presented here has been able to successfully predict the photochemical degradation kinetics of IBP and CBZ observed in the epilimnion of Lake Greifensee (Switzerland).[85,86]

3.4.8 Photo-transformation intermediates

It is also possible to model the formation rate constants and yields of intermediates. For instance, acridine (ACR) is a mutagenic compound that is formed from CBZ upon direct photolysis (yield η_{ACR}^{Phot} = 0.036, *i.e.* 3.6%) and $^{\bullet}$OH reaction (yield $\eta_{ACR}^{^{\bullet}OH}$ =0.031).[86] In the generic process *p*, CBZ could produce ACR with yield η_{ACR}^{p}, experimentally determined as the ratio between the initial formation rate of ACR and the initial transformation rate of CBZ.[86] The pseudo-first order rate constant of ACR formation in the generic process *p* is $(k_{ACR}^{p})' = \eta_{ACR}^{p} k_{CBZ}^{p}$. Therefore, the overall rate constant of ACR formation upon direct photolysis and $^{\bullet}$OH reaction of CBZ is:

$$(k_{ACR})' = \eta_{ACR}^{Phot} k_{CBZ}^{Phot} + \eta_{ACR}^{^{\bullet}OH} k_{CBZ}^{^{\bullet}OH} \qquad (76)$$

One can also obtain the overall yield of ACR formation from CBZ (η_{ACR}), as $\eta_{ACR} = (k_{ACR})'(k_{CBZ})^{-1}$, where k_{CBZ} is the overall rate constant of CBZ photochemical transformation ($k_{CBZ} = \sum_p k_{CBZ}^{p}$).

Figures 23 and 24 report $(k_{ACR})'$ and η_{ACR}, respectively, as a function of depth and NPOC. It can be observed that $(k_{ACR})'$ decreases with both *d* and NPOC, because ACR is formed from CBZ upon photolysis and $^{\bullet}$OH reactions that are both inhibited at higher depth (due to reduced sunlight irradiance) and at high NPOC (because of competition for irradiance between CDOM and CBZ and of $^{\bullet}$OH scavenging by DOM, respectively). The yield η_{ACR} also decreases with *d* and NPOC, but more slowly than $(k_{ACR})'$. This happens because direct photolysis and $^{\bullet}$OH reaction are the main CBZ transformation processes over a wide range of *d* and NPOC conditions, although the respective rates decrease with increasing *d* and NPOC. Reaction between CBZ and ^{3}CDOM*, which does not yield ACR [86] plays a significant role only at elevated *d* and NPOC, where its effect in the decrease of η_{ACR} can be noticed.

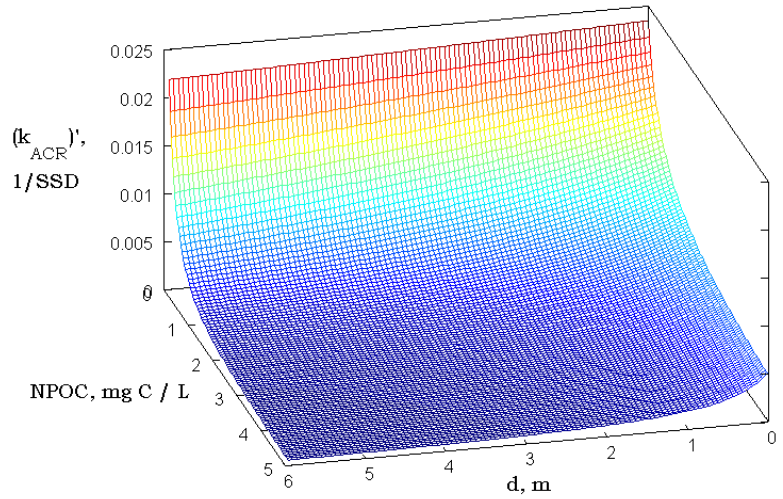

Figure 3.23. First-order rate constant of ACR formation, as a function of NPOC and depth *d*, with constant 50 µM nitrate, 1 µM nitrite, 2 mM bicarbonate and 10 µM carbonate.

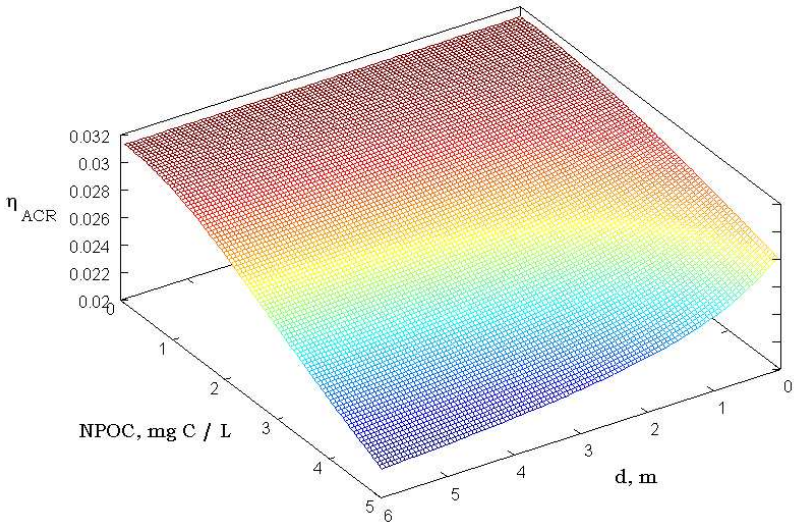

Figure 3.24. Yield of ACR formation from CBZ, as a function of NPOC and depth *d*, with constant 50 µM nitrate, 1 µM nitrite, 2 mM bicarbonate and 10 µM carbonate.

References

[1] C. Richard C, A. Ter Halle, O. Brahmia, M. Malouki, S. Halladja, Catal. Today 124 (2007) 82–87.

[2] J. G. Calvert, J. N. Pitts, Photochemistry. John Wiley & Sons, New York, 1966; pp 780-786.

[3] A. Bedini, E. De Laurentiis, B. Sur, V. Maurino, C. Minero, M. Brigante, G. Mailhot, D. Vione, Photochem. Photobiol. Sci. 11 (2012) 1445-1453.

[4] P. Boule, D. W. Bahnemann, P. K. J. Robertson (Eds.), The Handbook of Environmental Chemistry Vol. 2-M (Environmental Photochemistry Part II). Springer, Berlin, 2005.

[5] S. Chiron, C. Minero, D. Vione, Environ. Sci. Technol. 40 (2006) 5977-5983.

[6] D. Vione, S. Khanra, R. Das, C. Minero, V. Maurino, M. Brigante, G. Mailhot, Wat. Res. 44 (2010) 6053-6062.

[7] J. F. Endicott, G. Feraudi, J. R. Barber, J. Phys. Chem. 79 (1975) 630-643.

[8] A. Mallakin, D. G. Dixon, B. M. Greenberg, Chemosphere 40 (2000) 1435-1441.

[9] M. Jang, S. R. McDow, Environ. Sci. Technol. 29 (1995) 2654-2660.

[10] R. Dabestani, J. Higgin, D. M. Stephenson, I. N. Ivanov, M. E. Sigman, J. Phys. Chem. B 104 (2000) 10235-10241.

[11] V. Maurino, D. Borghesi, D. Vione, C. Minero, Photochem. Photobiol. Sci. 7 (2008) 321-327.

[12] M. E. Sigman, J. T. Barbas, S. Corbett, Y. Chen, I. N. Ivanov, R. J. Dabestani, J. Photochem. Photobiol. A: Chem. 138 (2001) 269-274.

[13] M. Brunke, T. Gonser, Freshwat. Biol. 37 (1997) 1-33.

[14] M. Czaplicka, Sci. Total Environ. 322 (2004) 21-39.

[15] M. A. Crespin, M. Gallego, M. Valcarcel, J. L. Gonzalez, Environ. Sci. Technol. 35 (2001) 4265-4270.

[16] C. Papaefthimiou, M. D. Cabral, C. Mixailidou, C. A. Viegas, I. Sa-Correia, G. Theophilidis, Environ. Toxicol. Chem. 23 (2004) 1211-1218.

[17] H. C. Zhang, C. H. Huang, Environ. Sci. Technol. 37 (2003) 2421-2430.

[18] D. E. Latch, J. L. Pacher, B. L. Stender, J. VanOverbeke, W. A. Arnold, K. McNeill, Environ. Toxicol. Chem. 24 (2005) 517-525.

[19] C. Guyon, P. Boule, J. Lemaire, New J. Chem. 8 (1984) 685-692.

[20] D. Vione, C. Minero, F. Housari, S. Chiron, Chemosphere 69 (2007) 1548-1554.

[21] F. Bonnichon, C. Richard, G. Grabner, Chem. Commun. (2001) 73-74.

[22] A. Zertal, T. Sehili, P. Boule, J. Photochem. Photobiol. A: Chem. 146 (2001) 37-48.

[23] L. Meunier, E. Gauvin, P. Boule, Pest. Manag. Sci. 58 (2002) 845-852.

[24] L. Comoretto, B. Arfib, S. Chiron, Sci. Total Environ. 380 (2007) 124-132.

[25] J. P. Aguer, F. Blachère, P. Boule, S. Garaudee, C. Guillard, Int. J. Photoenergy 2 (2000) 81-86.

[26] C. Tixier, H. P. Singer, S. Canonica, S. R. Müller, Environ. Sci. Technol. 36 (2002) 3482-3489.

[27] D. E. Latch, J. L. Packer, W. A. Arnold, K. McNeill, J. Photochem. Photobiol. A: Chem. 158 (2003) 63-66.

[28] M. DellaGreca, M. Brigante, M. Isidori, A. Nardelli, L. Previtera, M. Rubino, F. Temussi, Environ. Chem. Lett. 1 (2004) 237-241.

[29] M. Brigante, M. DellaGreca, L. Previtera, M. Rubino, F. Temussi, Environ. Chem. Lett. 2 (2005) 195-198.

[30] M. W. Lam, S. A. Mabury, Aquat. Sci. 67 (2005) 177-188.

[31] D. Vogna, R. Marotta, R. Andreozzi, A. Napolitano, M. D'Ischia, Chemosphere 54 (2004) 497-505.

[32] M. DellaGreca, M. R. Iesce, L. Previtera, M. Rubino, F. Temussi, Environ. Chem. Lett. 2 (2004) 155-158.

[33] M. Cermola, M. DellaGreca, M. R. Iesce, L. Previtera, M. Rubino, F. Temussi, M. Brigante, Environ. Chem. Lett. 3 (2005) 43-47.

[34] D. Vione, R. Das, F. Rubertelli, V. Maurino, C. Minero, S. Barbati, S. Chiron, Intern. J. Environ. Anal. Chem. 90 (2010) 258-273.

[35] E. M. White, P. P. Vaughan, R. G. Zepp, Aquat. Sci. 65 (2003) 402-414.

[36] J. M. Allen, S. Lucas, S. K. Allen, Environ. Toxicol. Chem. 15 (1996) 107-113.

[37] D. Vione, G. Falletti, V. Maurino, C. Minero, E. Pelizzetti, M. Malandrino, R. Ajassa, R.I. Olariu, C. Arsene, Environ. Sci. Technol. 40 (2006) 3775-3781.

[38] B. Sur, M. Rolle, C. Minero, V. Maurino, D. Vione, M. Brigante, G. Mailhot, Photochem. Photobiol. Sci. 10 (2011) 1817-1824.

[39] G. V. Buxton, C. L. Greenstock, W. P. Helman, A. B. Ross, J. Phys. Chem. Ref. Data 17 (1988) 513-886.

[40] P. Wardman, J. Phys. Chem. Ref. Data 17 (1989) 1027-1717.

[41] P. Neta, R. E. Huie, A. B. Ross, J. Phys. Chem. Ref. Data 17 (1988) 1027-1228.

[42] C. Minero, V. Maurino, E. Pelizzetti, D. Vione, Environ. Sci. Pollut. Res. 13 (2006) 212-214.

[43] S. Canonica, T. Kohn, M. Mac, F. J. Real, J. Wirz, U. Von Gunten, Environ. Sci. Technol. 39 (2005) 9182-9188.

[44] M. Minella, M. Rogora, D. Vione, V. Maurino, C. Minero, Sci. Total. Environ. 409 (2011) 3463-3471.

[45] R. C. Bouillon, W. L. Miller, Environ. Sci. Technol. 39 (2005) 9471-9477.

[46] P. R. Maddigapu, M. Minella, D. Vione, V. Maurino, C. Minero, Environ. Sci. Technol. 45 (2011) 209-214.

[47] S. Canonica, U. Jans, K. Stemmler, J. Hoigné, Environ. Sci. Technol. 29 (1995) 1822-1831.

[48] S. Canonica, M. Freiburghaus, Environ. Sci. Technol. 35 (2001) 690-695.

[49] V. Maurino, A. Bedini, D. Borghesi, D. Vione, C. Minero, Phys. Chem. Chem. Phys. 13 (2011) 11213-11221.

[50] P. R. Maddigapu, A. Bedini, C. Minero, V. Maurino, D. Vione, M. Brigante, G. Mailhot, M. Sarakha, Photochem. Photobiol. Sci. 9 (2010) 323-330.

[51] S. Canonica, H. U. Laubscher, Photochem. Photobiol. Sci. 7 (2008) 547-551.

[52] J. Wenk, S. Canonica, Environ. Sci. Technol. 46 (2012) 5455-5462.

[53] M. Czaplicka, J. Hazard. Mater. B134 (2006) 45–59.

[54] D. Vione, D. Bagnus, V. Maurino, C. Minero, Environ. Chem. Lett. 8 (2010) 193-198.

[55] A. L. Boreen, B. L. Edhlund, J. B. Cotner, K. McNeill, Environ. Sci. Technol. 42 (2008) 5492–5498.

[56] D. E. Latch, K. McNeill, Science 311 (2006) 1743–1747.

[57] M. Grandbois, D. E. Latch, K. McNeill, Environ. Sci. Technol. 42 (2008) 9184–9190.

[58] M. Minella, F. Romeo, D. Vione, V. Maurino, C. Minero, Chemosphere 83 (2011) 1480-1485.

[59] M. Minella, M. P. Merlo, V. Maurino, C. Minero, D. Vione, Chemosphere, in press. DOI: 10.1016/j.chemosphere.2012.07.013.

[60] L. Cavani, S. Halladja, A. Ter Halle, G. Guyot, G. Corrado, C. Ciavatta, A. Boulkamh, C. Richard, Environ. Sci. Technol. 43 (2009) 4348–4354.

[61] O. A. Trubetskoj, O.E. Trubetskaya, C. Richard, Wat. Res. 36 (2009) 518–524.

[62] S. Halladja, A. Ter Halle, J.-P. Aguer, A. Boulkamh, C. Richard, Environ. Sci. Technol. 41 (2007) 6066–6073.

[63] S. Chiron, S. Barbati, M. De Méo, A. Botta, Environ. Toxicol. 22 (2007) 222–227.

[64] Z. C. Heng, T. Ong, J. Nath, Mutat. Res., Genet. Toxicol. 368 (1996) 149–155.

[65] A. Tognazzi, A. M. Dattilo, L. Bracchini, C. Rossi, D. Vione, Intern. J. Environ. Anal. Chem., in press. DOI: 10.1080/03067319.2011.609932.

[66] A. Bedini, V. Maurino, C. Minero, D. Vione, Photochem. Photobiol. Sci. 11 (2012) 418-424.

[67] S. Chiron, C. Minero, D. Vione. Environ. Sci. Technol. 41 (2007) 3127-3133.

[68] J. Mack, J. R. Bolton, J. Photochem. Photobiol. A: Chem. 128 (1999) 1-13.

[69] D. Vione, V. Maurino, C. Minero, E. Pelizzetti, Environ. Sci. Technol. 36 (2002) 669-676.

[70] J. T. Cullen, B. A. Bergquist, J. W. Moffett, Mar. Chem. 98 (2006) 295-303.

[71] P. R. Maddigapu, C. Minero, V. Maurino, D. Vione, M. Brigante, G. Mailhot, Chemosphere 81 (2010) 1401-1406.

[72] S. Chiron, L. Comoretto, E. Rinaldi, V. Maurino, C. Minero, D. Vione, Chemosphere 74 (2009) 599-604.

[73] P. R. Maddigapu, D. Vione, B. Ravizzoli, C. Minero, V. Maurino, L. Comoretto, S. Chiron, Environ. Sci. Pollut. Res. 17 (2010) 1063-1069.

[74] C. Minero, S. Chiron, G. Falletti, V. Maurino, E. Pelizzetti, R. Ajassa, M. E. Carlotti, D. Vione, Aquat. Sci. 69 (2007) 71-85.

[75] C. Minero, V. Lauri, V. Maurino, E. Pelizzetti, D. Vione, Ann. Chim. (Rome) 97 (2007) 685-698.

[76] S. E. Braslavsky, Pure Appl. Chem. 79 (2007) 293-465.

[77] R. Frank, W. Klöpffer, Chemosphere 17 (1988) 985-994.

[78] D. Vione, S. Khanra, S. Cucu Man, P. R. Maddigapu, R. Das, C. Arsene, R. I. Olariu, V. Maurino, C. Minero, Wat. Res. 43 (2009) 4718-4728.

[79] D. Vione, J. Feitosa-Felizzola, C. Minero, S. Chiron, Wat. Res. 43 (2009) 1959-1967.

[80] D. Vione, M. Minella, C. Minero, V. Maurino, P. Picco, A. Marchetto, G. Tartari, Environ. Chem. 6 (2009) 407-415.

[81] D. Vione, V. Maurino, C. Minero, M. E. Carlotti, S. Chiron, S. Barbati, C. R. Chimie 12 (2009) 865-871.

[82] S. Chiron, S. Barbati, S. Khanra, B. K. Dutta, M. Minella, C. Minero, V. Maurino, E. Pelizzetti, D. Vione, Photochem. Photobiol. Sci. 8 (2009), 91-100.

[83] D. Vione, R. Das, F. Rubertelli, V. Maurino, C. Minero, In: Ideas in Chemistry and molecular Sciences: Advances in Synthetic Chemistry. B. Pignataro (ed.), Wiley-VCH, Weinheim, Germany, 2010, pp. 203-234.

[84] F. Al-Housari, D. Vione, S. Chiron, S. Barbati, Photochem. Photobiol. Sci. 9 (2010) 78-86.

[85] D. Vione, P.R. Maddigapu, E. De Laurentiis, M. Minella, M. Pazzi, V. Maurino, C. Minero, S. Kouras, C. Richard, Wat. Res. 45 (2011) 6725-6736.

[86] E. De Laurentiis, S. Chiron, S. Kuoras-Hadef, C. Richard, M. Minella, V. Maurino, C. Minero, D. Vione, Environ. Sci. Technol. 46 (2012) 8164-8173.